Lawrence Berkeley National Laboratory
Recent Work

Title
PHOTOMESONS FROM DEUTERIUM

Permalink
https://escholarship.org/uc/item/4mp7j1cp

Author
White, Robert Stephen

Publication Date
1951-05-24

eScholarship.org Powered by the California Digital Library
University of California

UNCLASSIFIED

UCRL- 1319

Copyright UCRL 1278

UNIVERSITY OF CALIFORNIA — BERKELEY

TWO-WEEK LOAN COPY

This is a Library Circulating Copy which may be borrowed for two weeks. For a personal retention copy, call Tech. Info. Division, Ext. 5545

RADIATION LABORATORY

DISCLAIMER

This document was prepared as an account of work sponsored by the United States Government. While this document is believed to contain correct information, neither the United States Government nor any agency thereof, nor the Regents of the University of California, nor any of their employees, makes any warranty, express or implied, or assumes any legal responsibility for the accuracy, completeness, or usefulness of any information, apparatus, product, or process disclosed, or represents that its use would not infringe privately owned rights. Reference herein to any specific commercial product, process, or service by its trade name, trademark, manufacturer, or otherwise, does not necessarily constitute or imply its endorsement, recommendation, or favoring by the United States Government or any agency thereof, or the Regents of the University of California. The views and opinions of authors expressed herein do not necessarily state or reflect those of the United States Government or any agency thereof or the Regents of the University of California.

UCRL-1319

UNIVERSITY OF CALIFORNIA

Radiation Laboratory

Contract No. W-7405-eng-48

Photomesons from Deuterium

Robert Stephen White

(Thesis)

May 24, 1951

Berkeley, California

Table of Contents

		page
I.	Abstract	4
II.	Introduction	5
III.	Experimental Procedure	9
	A. Target	10
	B. Gas Pumping System	12
	C. Collimators and Slits	12
	D. Absorbers	14
	E. Detectors	15
	1. Crystal Coincidence Detection	16
	2. Photographic Emulsion Detection	18
	F. Photon Beam Monitor	21
IV.	Validity of π Meson Identification	22
	A. Coincidence Crystal Detection	22
	B. Nuclear Emulsion Detection	23
V.	Analysis of Data	27
	A. Minus-Plus Ratio	27
	B. Cross Sections	28
VI.	Corrections	31
	A. Decay in Flight	31
	B. Slit Penetration	32
	C. Multiple Scattering	33
	D. Nuclear Interactions in Absorbers	34
	E. Line Source	35
	F. Photon and Meson Energy Loss in the Target	35
VII.	Results	36
	A. Minus-Plus Ratio for Deuterium	36

Table of Contents (Cont'd.)

B. Energy Distributions from Hydrogen and Deuterium at 135°, 90° and 45°. 37

C. Differential Cross Sections 38

D. Total Cross Sections 39

E. Ratios of Cross Sections of Deuterium to Hydrogen 40

VIII. Conclusions 41

IX. Acknowledgments 45

X. References 46

XI. Illustrations 48

I. ABSTRACT

Photons of a maximum energy of 312 ± 15 Mev in the "spread-out" bremsstrahlung beam of the Berkeley electron synchrotron have been used to produce charged mesons from deuterium and hydrogen. The gas was bombarded in a high-pressure, low-temperature target at a pressure of 140 atmospheres and a temperature of 77°K. The π mesons that were produced were collimated at 45°, 90° and 135° to the photon beam direction. π^+ mesons were detected by scintillation crystals, using π-μ, π-β, and π-μ-β coincidence detection. π^+ and π^- mesons were detected with nuclear emulsions. The ratio of the number of π^- to π^+ mesons produced from deuterium has been obtained as a function of the meson energy at an angle of emission of 45°. The mean values of the minus-plus ratio at 45° and 90° are 0.96 ± 0.11, and 0.98 ± 0.14, respectively. Energy distributions for π^+ mesons in cm^2, per Mev, per steradian, per "equivalent quantum," per proton have been obtained from hydrogen and deuterium at 135°, 90° and 45° and for π^- mesons from deuterium at 45°. Ratios of these cross sections for meson production from deuterium and hydrogen have been calculated. Differential cross sections at each of these angles have been obtained by integrating under the energy distribution curves. Ratios of the differential cross sections for π^+ mesons from deuterium and hydrogen are given. Total cross sections for π^+ meson production from deuterium and hydrogen have been obtained and the ratio of the total cross sections is given. The experiment is in qualitative agreement with the theory of Chew and Lewis but the statistics are not sufficient to determine the spin flip probability.

II. INTRODUCTION

The discovery of charged π mesons in 1947 by the Bristol group[1] led to a new approach in the study of nuclear interactions. π mesons have been used in production, scattering and absorption experiments for investigating these interactions. The earliest information concerning meson production came from cosmic-ray experiments. With the discovery[2] that π mesons could be made by bombardment of targets with particles from modern accelerators, it became feasible to undertake experiments under more controlled conditions. The production of π mesons by photons was definitely established by McMillan and Peterson[3] when they observed mesons from targets placed in the bremsstrahlung beam of the 322 Mev Berkeley synchrotron. Further experiments by McMillan, Peterson and White,[4] and by Peterson, Gilbert and White,[5] using nuclear emulsion detection with carbon as the target, established the ratio of the number of π^- to π^+ mesons produced as 1.3. This value was fairly independent of the energy of the mesons or the angle to the beam at which they were observed. Energy distributions and differential cross sections were obtained at each of the angles, 45°, 90°, and 135° to the beam direction. The total cross section for the production of the sum of π^+ and π^- mesons was found to be $4.0 \pm 1.6 \times 10^{-28}$ cm^2 per nucleus per "equivalent quantum." The number of "equivalent quanta," Q, is defined as the total energy in the beam divided by the maximum photon energy.[6] The production of μ meson pairs in the target was estimated to be less than 2 percent of the cross section for π meson production.

Littauer and Walker[7] have recently measured the minus-plus ratios of photomesons from a number of light isotopes and the ratios of the production cross sections to those from hydrogen at a meson energy of

50 Mev and at an angle of emission of 135° to the photon beam direction. They find a minus-plus ratio for carbon of 1.06. Camac, et al.,[8] for mesons of 65 Mev and meson angle of emission of 135° find a value of 1.1. These values are in good agreement with the value of Peterson, et al. when data is selected for the above angle and energy and is only slightly outside the standard deviation of the overall value of 1.3.

The experiments in which mesons are produced from photons bombarding targets involve simpler interactions than those of particle bombardment, and thus should be more subject to theoretical interpretation. Brueckner's[9] theoretical calculations indicate that the above minus-plus ratio cannot be explained solely by the interaction of the photon with the currents of the moving particles, as this gave a minus-plus ratio which is dependent on the energy and the angle of emission of the meson. However, when he used an interaction with the anomalous magnetic moments of the nucleons, he obtained a minus-plus ratio which was essentially one, independent of angle and energy.

Cook[10] has studied the photo production of π^+ mesons from hydrogen using photographic emulsions for detection. Bishop, Steinberger and Cook,[11,12] investigating this reaction, made use of the β^+ decay of the μ^+ meson to detect the π^+ mesons with scintillation crystals. They found an excitation curve which rises steeply for low photon energies then appears to level off at energies approaching 250 Mev. Their curve for the angular distribution of mesons from 250 Mev photons, in the center of mass system, appears fairly isotropic but increasing toward backward angles. A simple photoelectric effect, or the scalar meson theory would give a dipole distribution that would peak forward of 90° because of the retardation terms. Calculations by Brueckner[9] indicate

that the pseudoscalar theory should give a roughly isotropic angular distribution; however, his values decrease as the angle increases contrary to experiment.

The photoproduction of π^+ mesons as a function of A, the atomic number, has been measured by Mozley.[13] The number produced per nucleon in the target may be approximately fitted by an $A^{-1/3}$ curve. Littauer and Walker[7] have arrived at the same conclusion but obtained better agreement if the sum of π^+ and π^- mesons is plotted as a function of A. They have also found deviations from a minus-plus value of one. This deviation is especially prominent in Ca^{40} which has an even number of protons and neutrons. They find the value 0.58 for this minus-plus ratio. From Be^9 these investigators find a value of 2.4 for the minus-plus ratio, which is in agreement with the value of 2.2 of Medicus.[14] The higher neutron-proton ratio in the nucleus is not sufficient to explain this value, but, in addition, the loosely bound neutron must be more active in the production of mesons than the other nucleons. Jakobson[15] has recently measured the π^+ photomeson production from He at 45°, 90° and 135° to the beam direction and has measured the minus-plus ratio at 45°.

It is quite probable that production experiments with isotopes of a large number of nucleons yield more information about the structure of the nucleus, and the meson interaction with nucleons before leaving the nucleus, than about the initial act of the production of the meson itself. For information concerning the production act, therefore, one should do experiments with light isotopes. It would be interesting to study the π^- mesons from photons on free neutrons in order to get a comparison with the information that now exists concerning the production of π^+ mesons from free protons.[11,12] As a target of free neutrons is not

available, one may utilize the almost free neutron which exists in the deuteron. As the radius of the deuteron is quite large, the meson production should be fairly independent of the structure of the nucleus and of the absorption of the mesons that seems to occur in heavier nuclei.

Feshbach and Lax[16] have pointed out that unless the spin of the proton flips in the production of a meson and neutron in photon bombardment of deuterium, the production cross section will be down relative to the free proton cross section. From the reaction of a photon on a deuteron which makes two neutrons and a π^+ meson, if the deuteron is initially in the ^3S state.

$$h\upsilon + D \longrightarrow 2n + \pi^+$$
$$\longrightarrow 2p + \pi^-$$
$$^3S \qquad ^1S,\ ^3P$$

it is immediately seen that the resulting neutrons can only end in the ^1S, ^3P, ... states. The final state must be antisymmetric from the Pauli exclusion principle. If the final space state is symmetric, the spin state must be antisymmetric and vice versa. Unless the proton in the deuteron flips its spin in the reaction, the available phase space is reduced and the cross section is down relative to the cross section for production from a free proton. Chew and Lewis[17] have added that the ratio will be further reduced by an amount dictated by the binding energy of the deuteron. Using a phenomenological approach, they have calculated the ratio of the production cross sections from deuterium and hydrogen. Two constants appear that can be determined experimentally by a measurement of the ratios of the cross sections. These constants are the amplitude for spin flip and the amplitude for non-spin flip.

An exploratory experiment of Mozley and White,[18] using light and

heavy water targets and electronic meson detection,[11,13] indicated that the π^+ meson production from deuterium did not differ greatly from the π^+ meson production from hydrogen.

The present experiment was designed to investigate the production of π mesons from deuterium as a function of both angle of emission and π meson energy, and to measure the ratios of production cross sections for π^+ mesons from hydrogen and deuterium.

III. EXPERIMENTAL PROCEDURE

The source of photons for this experiment was the 312 ± 15 Mev bremsstrahlung "spread-out" beam from the Berkeley electron synchrotron. This beam was generated from the 322 ± 5 Mev electron beam which struck an internal 0.020-inch platinum target. The "spread-out" beam was obtained by modulating the rf accelerating voltage such that the electrons spill into the target over a period of about 3,000 μ sec.[48] This occurs in such a way that about half the electrons hit the target before and after peak field is reached. The resulting spread in the maximum photon energy is about ± 15 Mev. The emerging beam had a full width at half-intensity of 0.0135 radians. At 55 inches from the electron target the beam was defined by a one-inch tapered hole in a nine-inch lead wall, as is shown in Fig. 1. Two secondary collimators were used to absorb the spray of electrons scattered from the walls of the primary collimator. The first was a hole one inch in diameter and six inches long, the second, one and one-half inches in diameter and eight inches long, each bored from a lead block. The photon beam was 1.12 inches in diameter at the entrance to the gas target and 1.45 inches in diameter at the exit end. The target and collimators were aligned by means of a transit. Photographs of the beam confirmed the fact that

the target was aligned. The beam was monitored by means of an ionization chamber placed in front of the primary collimator. A second ionization chamber placed ten feet behind the rear end of the target was used as a check on the front monitor.

Mesons produced in the gas of the target were channeled by means of lead collimators and the nominal angles of 135°, 90° and 45° were defined by uranium slits. The meson energy was defined by lead absorbers. Mesons in the proper energy interval stopped and were detected either in nuclear emulsions or in coincidence crystal detectors. A photograph of the experimental set-up is shown in Fig. 2.

A. Target

Two types of targets were considered for this experiment. As the boiling point of hydrogen is 4°K lower than the boiling point of deuterium, one could use liquid hydrogen to liquefy deuterium for a liquid target. The alternative was to use a high-pressure, low-temperature gas target similar to the type used in the capture of π^- mesons.[19] The liquid type had the advantages of a higher deuterium density by a factor of two, and less stainless steel in the beam which can produce mesons and cause electron background. It could, therefore, be used as a point target. The high-pressure low-temperature target, however, had the great advantage of simplicity in design and for this reason was selected for the experiment.

The assembly of the target is shown in Fig. 3. The photon beam traversed 0.045 inch of stainless steel on each end of the target, 0.005 inch of vacuum wall and 0.040 inch of pressure wall. Mesons, produced in the gas of the target, which were emitted perpendicular to the axis of the target, had to penetrate a 0.080-inch pressure wall,

0.31 inch of liquid nitrogen, a 0.012-inch liquid nitrogen wall, and finally, a 0.027-inch vacuum wall. The minimum energy of π mesons that could penetrate this material was 22 Mev; at 45° and 135° the minimum energy was 27 Mev. The hemispherical end pieces were screwed on to the cylindrical center section so that the pressure exerted by the gas was transmitted to the screw threads. The gas seal was made by welding the end caps onto the center section. The pressure chamber was hydrostatically tested at room temperature to 240 atmospheres. Gas tests were made at a temperature of 77°K to 340 atmospheres. In actual usage the pressure was never allowed to exceed 150 atmospheres at 77°K so that one always had a tested safety factor of greater than two and a calculated safety factor of greater than four. In addition, two safety patches were inserted (as shown in Fig. 4) which would break at 220 atmospheres and allow the gas to expand into a cylinder of large volume.

The liquid nitrogen was stored in a tank above the target and fed to the cooling wall through pipes. Two thermocouples were placed in the tank at different levels and the signals were sent to an automatic recorder in the counting area so that one had a record of the levels at all times and could fill the tank when necessary. After equilibrium conditions had been reached, the nitrogen supply would last for at least four hours. A third thermocouple was placed on one of the end caps so that one also had a record of the temperature of the pressure wall, and thus the gas, at all times.

One tube from the gas pressure cylinder was led directly to the counting area to a calibrated pressure gauge. From this gauge the pressure of the gas was read at intervals. The number of target protons per cm^3 was obtained from the pressure-volume versus pressure curves of Johnston et al.[20] Their values are given to 0.1 percent

accuracy.

The vacuum system was for the purpose of lowering the heat conduction to the wall which was at room temperature, and for conserving the liquid nitrogen in the dewar. Without this vacuum system the walls of the target would ice to the point that the meson energies would be indeterminate. To obtain the vacuum of about 10^{-6} mm of Hg a 20-liter oil diffusion pump was used, backed by a Duo Seal fore pump. A photograph of the target, collimators and detectors is shown in Fig. 5.

B. Gas Pumping System

The gas pumping system is shown schematically in Fig. 4. The hydrogen pump was used to increase the pressure of the gas from cylinder pressure, about 115 atmospheres, to about 140 atmospheres. After using the hydrogen gas, it was discharged through a grounded hose to a safe distance outside the building. Because of the expense of the deuterium, it was necessary to recover it after each bombardment. The recovery system of Panofsky, et al.[19] was used for this purpose. The pressure system was pumped down to about 1 mm of Hg pressure in each gas exchange to insure negligible mixing of the gases. The change-over time to equilibrium conditions from a hydrogen bombardment to a deuterium bombardment was about one hour. The limitation on the speed of this operation was imposed by the speed of the deuterium oil pumping system. When comparison among gases was desired at least three changes of the gases were made in each 16-hour bombardment period.

C. Collimators and Slits

An element with a high nuclear charge, Z, is most effective in stopping electrons and photons in the bremsstrahlung and pair production region. For this reason Pb was selected for the collimating system.

Two sections through the lead collimating system are illustrated schematically in Figs. 6 and 7. Fig. 6 is a section perpendicular to the photon beam direction at the center of the target. Five identical collimating systems were arranged azimuthally about the beam direction. The lower collimating system was used only for the coincidence crystal detectors. The other four were used for the nuclear emulsion detection. Four identical collimating systems allow the simultaneous measurement of four different energies at each of the three angles of observation. This simultaneous exposure of emulsions is necessary for the conservation of beam time.

Fig. 7 is a plane section though one of the collimating systems. The three items that were most important in design of the collimating system were: a) a sufficiently large solid angle and length of target that statistics could be obtained in a reasonable length of time with the photon intensity available; b) enough angular discrimination so that the angles of emission of mesons that reach the detector are reasonably defined; and c) sufficient shielding against electrons that the meson signal can be detected above the electron background.

In the geometrical arrangement used, the angles as defined by the slits are given in Table I.

Table I. Angular resolution of the collimating systems.

Detector	Angle
Nuclear Emulsions	$45^\circ \begin{smallmatrix} + 17^\circ \\ - 15^\circ \end{smallmatrix}$
	$90^\circ \pm 16^\circ$
Crystal	$90^\circ \pm 16^\circ$
	$135^\circ \pm 19^\circ$

These angles may be combined with the expected r.m.s. multiple scattering angle calculated for mesons passing through lead and glass absorbers

from 70 Mev down to 200 microns from the end of their range (2 Mev). The resulting widths of the calculated meson distributions fit the observed distributions very nicely; this is illustrated for the nominal angles of 90° and 45° in Fig. 8. The calculations were based on the methods of Eyges[21] and Foldy[22] for scattering of particles while undergoing energy loss in absorbers. There is, of course, some penetration of the slits; however, this is small and corrections are made for this.

In order to minimize slit penetration, it is desirable to use a material which has a maximum stopping power per unit length. Uranium fits this specification. It was found that the low-energy gammas from the uranium did not contribute appreciably to the single-grain background on the nuclear emulsions, nor to background counts in the crystals. In addition, if the slits are placed far apart, for this experiment two inches, the slit penetration is decreased and the solid angle and length of target observed are increased. This, however, is at the expense of angular resolution. The part of the emulsion scanned was in the shadow of the slits, as was most of the crystal in which the mesons stopped, so very few electrons or mesons could be reflected at small angles off the slits into the detectors. The slit was also cut away on the back side, the side nearest the detector, so that only electrons or mesons reflected from it at large angles could reach the detectors.

D. Absorbers

An absorber material is desired that has a large stopping power per unit length and introduces a minimum of multiple scattering of the mesons. In addition, since many high energy electrons are made in the

ends of the stainless steel target and are then scattered into the detectors from the cylindrical walls of the target, they must be either attenuated before reaching the detector or allowed to pass through unaffected with the hope they will not contribute to the background of the detector. Three possible absorber materials are Al, Cu and Pb, which have "radiation lengths" for fast electrons of about 10, 1.5 and 0.5 cm. Al can be immediately rejected because of its low stopping power per unit length. Cu is slightly better than lead for the first qualification, and certainly better for the second. Either Cu or Pb absorbers must be as thick as 8 cm in order to stop the high energy mesons. This is a distance of several radiation lengths, even for copper. The alternative of allowing the electrons and photons to pass, unhindered, was abandoned in favor of the method of rapid degradation of the energy of the electrons and photons. Pb was selected for this reason although it does introduce more multiple scattering than Cu. There is an additional reason for selecting lead. If the cross section for nuclear interactions of mesons in the absorbers is a nuclear area, lead will have less nuclear interaction per unit stopping power than copper.

The energies of the π mesons that stopped in the detectors was determined from the range-energy curves of Aron, et al.,[23] and the range-energy curve for glass and emulsion.[24,25]

E. Detectors

When photons strike deuterons, both π^+ and π^- mesons are produced. Some of these mesons are slowed down and will stop in the detector. There is good evidence that in the presence of matter π^- mesons are almost invariably captured after coming to rest as several thousand π^-

meson endings have been observed in emulsions without conclusive evidence of a π-μ ending.[26] π^+ mesons, on the other hand, are repulsed by the coulomb field of the nucleus and will decay into μ^+ mesons with a characteristic mean life of 2.6×10^{-8} sec.[27,28] These decay μ mesons have an energy of about 4 Mev and, in turn, decay into positrons with a mean life of 2.1×10^{-6} sec.[29] These properties were used to identify both π^+ and π^- mesons in nuclear emulsions from the tracks left by the ionizing particles. There are many electronic meson detection systems which use some combination of $H\rho$, Range, pulse height, time of flight, and decay property of the π^+ and μ^+ meson. For this experiment the π^+-μ^+ coincidence detection scheme of Jakobson, Schulz and Steinberger,[28] the β decay of the μ^+ meson, called π-β coincidence detection, used by other experimenters,[11,29] and coincidences between these schemes, called π-μ-β detection, were chosen for detection of π^+ mesons. The coincidence crystal detection was used for detailed statistics of the energy distribution, and the nuclear emulsions for fixing absolute cross sections and for determination of the deuterium minus-plus ratio.

1. Crystal coincidence detection. Some of the π^+ mesons leave the target, pass through the absorber and first crystal and stop in the second crystal, as illustrated in the block diagram of electronics, Fig. 9. If such an event occurs, a scintillation from each of the crystals is observed by its photomultiplier. The individual signals are signals are sent to a Wiegand-type distributed coincidence.[30] If the signals occur in a time separated by less than 10^{-8} sec., the resulting coincidence signal is delayed by the desired amount of RG63/U cable and is then used to open a gate of 8×10^{-8} sec. If the π^+ meson decays into a μ^+ meson during the time interval that the gate is open, a coincidence occurs in the π^+-μ^+ distributed coincidence circuit, and a π^+-μ^+ meson

is registered on scaler 2. In a similar manner, the π^+-π^+ pulse may be used to open a series of β^+ gates. The beta coincidences are registered on scalers 7, 8, 9 and 10. As the μ^+-β^+ decay mean life is 2×10^{-6} sec., shaping circuits can be used along with the slower coincidence circuits. The first beta gate may be put into coincidence with the π-μ signal to form the π-μ-β coincidence.

The best data were collected from the π-μ coincidence as the background from the π-β was high and the counting rate from the π-μ-β low. The beam level was set for most efficient counting with the π-μ coincidences and except at low meson energies, thin absorbers, the photon beam could be held to its maximum level. The spread-out beam of the synchrotron, about 3,000 microseconds, was used to increase the duty cycle. As the electrons are peeled off before, during and after peak magnetic field the spread-out beam has a slightly lower peak mean photon energy, 312 ± 15 Mev, than the spiked beam, 322 ± 5 Mev.

Different counting methods were used to count the same events; therefore, it would appear possible to determine the efficiencies of each of the three methods and the actual number of π^+ mesons that stopped in the crystal. This determination is dependent on the fact that all π^+ mesons stopping in the second crystal must open gates. Counting rate versus photomultiplier voltage curves were run for the stopping crystal but no clear-cut π meson plateaus were observed. The efficiencies were, therefore, calculated from the nuclear emulsion data and this determination showed that at the photomultiplier voltages used, 1200 v, only about half the π^+ mesons stopping in the last crystal opened gates. The measured efficiencies and the typical ratios of the background counts to true counts are given in Table II. The counting rate for the π-μ coincidences was of the order of one per minute at

Table II. Crystal coincidence detection efficiencies and background

Detection Method	Efficiency	Background Counts / True Counts
π-β	0.27	2 - 5
π-μ	0.077	0.10 - 0.20
π-μ-β	0.027	$\sim$0.01

the nominal angle to the beam of 90° and at energies of about 70 Mev. The background counting rates were compatible with those calculated from the number of gates opened, the singles counting rate, the duty cycle, and length of the gates. Additional information concerning the counting techniques is available.[28,15]

2. Photographic emulsion detection. Ilford C-2 nuclear emulsions were selected for exposure as their sensitivity is about optimum for meson detection. The sensitivity is low enough that the π meson tracks show a rapid grain density change in the last two hundred microns of track length, yet high enough that the lightly ionizing μ mesons can be identified on the ends of π mesons. The large amount of multiple scattering near the meson ending is an additional aid in identifying the mesons. Certain types of mesons have endings which make identification easier. When meson track endings are observed under a microscope, three distinct types are noted: 1) π-μ, a meson leaving the ending. This event was surely a π^+ meson decaying into a μ^+ meson. 2) σ, one or more ionizing particles leaving the ending. This event is certainly a π^- meson which was captured by a nucleus of the emulsion. 3) ρ, nothing leaving the ending. This event could be a π^- meson which was captured in a nucleus of the emulsion and one or more neutrons were emitted, a μ^+ meson from the decay at rest of a π^+ meson outside the

emulsion, a μ^+ or μ^- meson from decay in flight of a π^+ or π^- meson.

The number of π^+ mesons ending in the emulsion is certainly equal to the number of π^+-μ^+ endings as π^- mesons at rest in emulsions very seldom, if ever, decay.[26] There is good evidence that a negligible number, if any, of the π^+ mesons decay directly into positrons.[31,32]

The number of π^- mesons ending in the emulsion is equal to 1.37 times the number of σ endings observed, as data on magnetically sorted π^- mesons show that 0.73 ± 0.02 of the π^- mesons form stars.[33] This number has been verified within statistics by Peterson, et al.[5]

The track ending of a μ^+ meson is always of the ρ type because it always decays into a positron,[34] and Ilford C-2 emulsions are not sensitive enough to record electron tracks. Jones and White,[35] in an experiment with π^- mesons produced from alpha-particles on carbon, found a region in their emulsion in which only μ^- mesons, from decay in flight of π^- mesons, were located. They were able to put a limit of $\pm 0.07 \pm 0.03$ on the number of μ^- mesons which form stars. Recently George and Evans,[36] from studies of nuclear emulsions exposed underground, found that 0.055 ± 0.011 of the μ^- mesons that stop in their emulsions produce stars. As there is evidence, to be discussed later, that no μ^- mesons are produced in the target, the only μ^- mesons which stop in the emulsion will be those from decay in flight. Since less than 0.05 of the π^- mesons decay in flight, the fraction of stars found in the emulsion due to μ^- mesons is negligible. The types of track endings of the four kinds of mesons are summarized in Table III.

Table III. Summary of track endings

Meson	Track Ending
π^-	σ_n n = (1, 2, 3, ...) = number of prongs
π^+	π-μ
μ^-	ρ, σ_n
μ^+	ρ

The nuclear emulsions were backed by 1 x 3 x 1/16 inch glass plates. They were exposed in lead boxes in stacks of five with eight glass plates on the top and bottom to guarantee a uniform stopping material. This method of exposure was economical of beam time as nuclear emulsions could be pulled at different exposures and blank glass plates inserted. The exposures ranged from 1 x 10^{12} to 5 x 10^{12} equivalent quanta. All emulsions exposed to the maximum number of photons were suitable for reading except for those which recorded the lowest energy mesons (no absorber energies). With emulsions exposed near the synchrotron beam the background limitations are imposed by the single grain background from the many electrons which traverse the emulsions. Although the emulsions used were not sensitive enough to record their tracks, the electrons make grains developable at intervals along their path and enough of these grains tend to fog the emulsions. The single grain background on the emulsions indicated that practically all of the electrons were coming from the target.

In order to obtain absolute cross sections, it was necessary to have a measurement of the emulsion thickness before development; if one knows the shrinkage factor and the thickness after development the original thickness is easily obtained. This shrinkage factor was found by sending 390 Mev alpha-particles through the emulsions at an angle of 45° to the plane of the emulsion. As the emulsions shrink only in the

dimension perpendicular to the plane of the emulsion, the projected track length after development is equal to the original thickness before development. The ranges of the alpha-particles and the thickness of the emulsion after development could be measured to an accuracy of greater than one percent and in certain regions of the emulsions the angle of the alpha-particle beam was known to about a degree, except for a few scattered alphas which could be discarded. However, in some of the developments the layers of emulsion slid relative to one another which caused the alpha-particle tracks to appear curved. Because of inaccuracies introduced by this warpage, the error in the shrinkage factor is estimated to be as large as 5 percent. The value used in this experiment was 2.42 ± 0.12. As all of the emulsions were taken from the same batch, and as all received the same development treatment, the relative thicknesses should be good to about 2 percent. An additional factor affecting the thickness was relative humidity on the day of bombardment by alpha-particles versus that on the days the plates were exposed to mesons. Very little is known about the thickness of the emulsions relative to the humidity conditions.

The total volume of emulsion scanned for the deuterium exposures was about 0.6 cm^3, for the hydrogen exposures about 0.4 cm^3.

F. Photon Beam Monitor

The photon beam was monitored by two ionization chambers, one placed before the primary collimator, the other placed 10 feet behind the target, as is shown in Fig. 1. The fore ionization chamber was used as the absolute monitor and the one aft as a check on the first. The ratios of the readings from the two chambers were essentially constant throughout the run. The fore chamber was calibrated by Blocker,

Kenney, and Panofsky,[37] and they estimate the absolute calibration to be good to better than 20 percent. The relative values as estimated from the ratios of the readings of the ionization chambers should be better than two percent. In order to minimize drifts in the monitors and detection equipment, the data was taken cyclically. When an energy distribution was being run, a given gas was left in the target and the absorbers (energies of the π^+ mesons being detected) were changed cyclically. When comparison among gases was desired, the energy was kept constant and the gases were changed. Also comparisons among angles were made in a like manner.

IV. VALIDITY OF π MESON IDENTIFICATION

As evidence that π mesons were, in truth, detected and that these mesons came from the gas of the target, the following facts are given.

A. Coincidence Crystal Detection

It will be first established that these detection methods do indeed detect π^+ mesons, and, second, that these mesons must have been produced in the gas of the target. 1) The π-μ detection equipment has been used successfully for obtaining the value of the π^+ meson mean life.[28] 2) This π-μ equipment[38] has been used for reproducing the "hydrogen peak" in the meson distribution curve from protons bombarding protons previously reported by Cartwright, et al.[39] 3) When the maximum photon beam energy was reduced below the threshold for meson production, the number of true counts approached zero but the background counts remained. 4) The shape of the π^+ meson energy distribution at 90° from photons on hydrogen compares well with the one obtained by Bishop, et al.[12] whose data was obtained from the π-β equipment.

5) The relative shapes of the distributions obtained by each of the counting methods agree within statistics at both 90° and 135° to the beam direction. 6) The ratio of the number of mesons produced from deuterium and hydrogen at an angle to the photon beam of 90° and meson energy of 70 Mev as determined by the coincidence crystal detection and by nuclear emulsion detection agree within statistics.

A run was made with the experimental setup identical to the usual runs except no gas was allowed in the pressure chamber. With the crystals in a position to detect 55 Mev mesons emitted at 90°, no counts were observed in a time in which 75 counts with the π-μ equipment would normally be observed. The number of mesons of this energy and angle of emission from the stainless steel target walls was therefore negligible.

B. Nuclear Emulsion Detection

It has previously been noted that at each of the nominal angles, 90° and 45°, the experimental angular distribution of mesons, 200 microns from their endings, fits the expected distribution. Therefore, these particles must have been emitted from the target and follow the multiple scattering distribution of mesons. In Fig. 10 the distribution of the various types of mesons with depth is shown. Near the surface of the emulsion, or near the glass, the tracks are shorter and therefore more difficult to identify. Also, if prongs or mesons are emitted from the ending there is a possibility that they will be missed. If one discards data within three microns (after development) from both the surface and the glass, the distribution is then constant within statistics and the identification is constant with depth in the emulsion. Only data meeting the above criterion was used. This step removed about 7 percent of the available emulsion volume.

In Fig. 11 is shown a plot of the lengths of the paths of the mesons, measured from their endings back to the point where they entered or left the emulsion. These ranges were measured to only about 10 percent accuracy. Again the distribution of ranges is that to be expected except for those mesons of a very short range. The distribution of μ^+ mesons from the ends of π^+ mesons lends itself rather easily to analysis. The expected distribution function for isotropic emission of μ^+ mesons from the ends of π^+ mesons has been plotted along with the observed distribution. The shape of the calculated distribution is not too sensitive to the exact thickness of the emulsion or to exact amount of emulsion that is rejected near the surface and glass. In the experimental plot are 520 mesons, 80 of which are complete. The complete μ^+ mesons are those which traveled their total range of 600 microns in the emulsion. The curve on the plot was normalized in the region of 50 to 500 microns. As π^+ mesons with very short μ^+ meson decays are certainly more difficult to find than those with long decay tracks or π-μ completes, the lack of μ^+ mesons in the 0-50 micron interval is to be expected. The curve fitted in this manner would predict 76 π-μ completes, well within the statistics of the 80 observed. It would also indicate that about 7 percent of the total π^+ mesons were not seen. The curve could also be normalized from 50 microns to infinity (all ranges above 600 microns would be included in the π-μ completes). This fit would predict 79 π-μ completes and would indicate that about 10 percent of the total π^+ mesons were missed.

Plots of the angular distribution of all types of mesons for the nominal angle of 45° are shown in Figs. 12 and 13. From the deuterium plot, one can see that the distribution of μ^+ mesons from π^+ endings is uniform in angle of emission. The π^+ and π^- mesons are certainly coming

from the target. The distribution of ρ mesons shows a uniform background of μ^+ mesons plus a hump from the target direction. If one subtracts from this distribution the uniform background of μ^+ mesons from decay at rest of π^+ mesons and the number of μ^+ and μ^- mesons due to decay in flight of the π mesons, the remaining number of ρ mesons must be from π^- mesons which do not form stars plus any μ mesons that might have been produced in the target. If all of the remaining mesons are considered π^- mesons which do not form stars, one arrives at the prong distribution of π^- mesons shown in Table IV. The data of Adelman and Jones, Menon, and Adelman,[40] has been included for comparison. If one takes their fraction of π^- mesons which do not form stars, the ratio of the cross section for μ meson production to π^+ meson production in the target is then -0.04 ± 0.08. Within statistics there were no μ mesons produced in the target; this value is in agreement with the experiment in which carbon was bombarded by photons.[5] The analysis of the hydrogen data, Fig. 13, gives a similar result. If, on the other hand, one assumes no μ mesons are made in the target, the experimental fraction of π^- mesons which give no ionizing tracks at their endings agrees within statistics with the value of Adelman.

There is some difficulty in distinguishing between π^+ mesons with very short decay μ^+ meson tracks and π^- mesons with one very lightly ionizing short prong. Analysis of magnetically sorted π^- mesons indicated that almost always a π^- meson with a lightly ionizing prong was accompanied by a "club," which is thought to be the recoil of the nucleus.[5] This criterion was used in identification with the resulting number of σ_1 mesons shown in Table IV. As this number agrees within statistics with the value of Adelman, et al.,[40] it is thought that the separation between π-μ and σ_1 mesons was made correctly. The prong

distribution of σ mesons also agrees, within statistics, with the values given in Table IV.

Table IV. Fractional number of prongs from σ mesons

	from 303 σ mesons	Adelman and Jones, Menon et al., Adelman from 3366 σ mesons
σ_0	0.23 $\pm$ 0.08	0.268 $\pm$ 0.021
σ_1	0.26 $\pm$ 0.03	0.237 $\pm$ 0.007
σ_2	0.28 $\pm$ 0.03	0.239 $\pm$ 0.007
σ_3	0.15 $\pm$ 0.02	0.163 $\pm$ 0.006
σ_4	0.06 $\pm$ 0.01	0.077 $\pm$ 0.004
σ_5	0.02 $\pm$ 0.01	0.014 $\pm$ 0.001
σ_6	0.003 $\pm$ 0.003	0.001 $\pm$ 0.001

In order to get true minus-plus ratios, the relative efficiencies for π^+ and π^- meson detection must be known. The previous discussion indicated that up to 10 percent of the π^+ mesons might not have been seen, or were classified with the ρ mesons, mainly because some of the short μ^+ meson prongs escaped unnoticed. Many short π^- mesons are slightly easier to identify because of the heavily ionizing tracks at their endings. However, some of these are confusable with the low-energy photon-induced stars in the emulsion and might be missed. In addition, there are probably a few missed which emit a very high energy proton that is not seen. In view of these arguments it is felt that the relative detection efficiencies are about equal, and if systematic errors are present it would tend to lower the minus-plus ratio slightly.

Most internal checks indicate that the absolute efficiencies of observers is greater than 90 percent. Since these absolute efficiencies are not known precisely, the data was not corrected for observer efficiency. In order to minimize observer error, the area of the emulsion

to be scanned was divided into two parallel strips, each 1 cm x 2.5 cm. Each area was scanned by a different observer. Comparing the data from the two areas showed no systematic error that could be attributed to either of the two observers who took data for this experiment.

Additional evidence was obtained from the hydrogen exposures which indicated that the detected mesons were coming from the gas of the target. At the nominal angle of 45° to the beam direction, 220 π-μ endings were observed and only 3 π endings. At 90°, 100 π-μ and 2 σ endings were seen. All of these σ mesons came from the target direction which indicates they were not cosmic-ray produced. It is thought that π^- mesons cannot be made from photons on protons. Since photons on stainless steel should give about as many π^+ as π^- mesons, it follows that the background of π^+ or π^- mesons from the target walls is less than 2 percent of the π^+ mesons from the hydrogen gas. On the other hand, if all of the mesons came from the gas in the target, one has the result that the number of π^- mesons produced from hydrogen is about 2 percent of the number of π^+ mesons; this alternative is considered quite improbable.

V. ANALYSIS OF DATA

A. Minus-Plus Ratio

A quantity which should be independent of beam monitoring, density of the bombarded gas, and geometry considerations is the minus-plus ratio. It is, however, dependent on the relative observer efficiencies for detection of π^- and π^+ mesons. In a particular π meson energy interval and angle of emission, the minus-plus ratio is simply:

$$\frac{[\pi^-]}{[\pi^+]} = \frac{1.37\ [\pi]}{[\pi - \mu]}$$

where $[\sigma]$, and $[\pi - \mu]$ are the numbers of σ and π-μ meson events found in the volume of emulsion corresponding to the particular π meson energy and angle.

An alternate, less reliable, method of obtaining the ratio is of interest in indicating experimental consistency. The total number of mesons observed in a given volume of emulsion is

$$[T] = [\pi\text{-}\mu] + [\sigma] + [\rho]$$

Since the number of μ^+ mesons observed in the volume of emulsion from decay of π^+ mesons at rest is equal to the number of π^+ mesons, and since no μ mesons are produced in the target, substitution into the above equation gives

$$\frac{[\pi^-]}{[\pi^+]} = \frac{2 + f_d}{\frac{0.73\ [T]}{[\sigma]} - (1 + f_d)}$$

where f_d is the fraction of μ mesons, from decay in flight of π mesons, which stop in the volume of emulsion.

The reason that this is a less reliable method is that the total number of mesons includes ρ endings which are more difficult to identify than π-μ or σ endings as there is no distinguishing event at their endings.

B. Cross Sections

For a line source emitting π mesons, in the case where there is only one other particle in the final state, e.g., photons bombarding protons to give a π^+ meson and a neutron, the differential cross section can be found from the following formula:

Figure 14

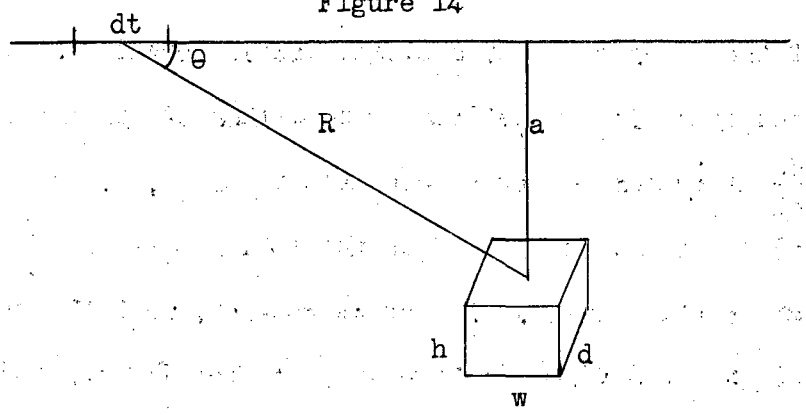

$$\frac{d\sigma(\bar{\theta},k)}{d\Omega} = \frac{1}{\epsilon} \frac{\Delta N}{hd\ G(\bar{\theta})\left(\frac{dq}{dk}\right)\left(\frac{dk}{dE}\right)\left(\frac{dE}{dR}\right) n}$$

where ϵ is the efficiency of the detector.

h is the effective height of the detector.

w is the effective width of the detector.

d is the effective length of the detector.

ΔN are the number of counts observed at a particular meson energy E, and average angle of emission, $\bar{\theta}$.

dq/dk are the number of quanta of energy k, which contribute to the production of the mesons. This factor depends on the detailed shape of the bremsstrahlung spectrum.

dk/dE relates the photon energy interval to the meson energy interval. This factor may be obtained from knowledge of $k = f(E,\bar{\theta})$

dE/dR relates the range interval of the detector to the energy interval of mesons leaving the target. It is a function of $\bar{\theta}$ and E.

n is the number of target particles per unit volume, in this experiment, either the number of protons or neutrons per unit volume.

$G(\bar{\theta}) = \iint \frac{dwdt}{R^2} = \frac{1}{a}\iint dwd\theta$ This is the geometrical factor that changes only in going from one average angle to another.

R is the distance from an interval of length of the target, dt, to the detector.

a is the perpendicular distance from the line source to the detector.

If there are more than two particles in the final state, the energy of the π meson is not a single valued function of the photon energy, and dk/dE is not defined. One method of evaluating data is to replace $\frac{dq}{dk}\,dk$ by the number of equivalent quanta, Q, where the number of equivalent quanta is defined as the total energy in the beam divided by the maximum photon energy. The cross section, with the number of equivalent quanta defined in this way, is then for crystal coincidence detection,

$$\frac{d^2\sigma\,(\bar{\theta},E)}{dE\;d\Omega} = \frac{1}{\epsilon}\,\frac{\Delta N}{hd}\,\frac{1}{G(\bar{\theta})}\,\frac{dR}{dE}\,\frac{1}{Qn}$$

for nuclear emulsion detection,

$$\frac{d^2\sigma\,(\bar{\theta}E)}{dE\;d\Omega} = \left(\frac{\Delta N}{\Delta V}\right)\frac{1}{g(\bar{\theta})}\left(\frac{dR}{dE}\right)\frac{1}{Qn}$$

where $(\Delta N/\Delta V)$ is the number of meson events recorded per unit volume of emulsion at a particular π meson energy E, and angle of emission $\bar{\theta}$, $g(\bar{\theta})$ equals $G(\bar{\theta})$ per unit width, w, of the emulsion.

The differential cross section can be found by integrating $\frac{d^2\sigma}{dE d\Omega}\,(\bar{\theta},E)$ over dE

$$\frac{d\sigma(\bar{\theta})}{d\Omega} = \int_0^{E_{max}} \frac{d^2\sigma}{dE\;d\Omega}\,dE$$

and the total cross section by integrating $d\sigma/d\Omega$ over $d\Omega$

$$\sigma_t = \int \frac{d\sigma}{d\Omega}\,d\Omega$$

The data must be extrapolated from 0 to 40 Mev to obtain the differential cross sections, and over the angles that were not measured to obtain the total cross sections.

It is worth noting that for a point source emitting mesons, the meson density at the detector is a volume effect alone and therefore independent of the size or orientation of the detector.

It is a property of a line source which emits isotropically that the number of events detected by a point detector per unit angle is independent of the angle from which they come. Therefore, at a given average collimator angle, $\bar{\theta}$, the geometry factors $G(\bar{\theta})$ or $g(\bar{\theta})$ will be constants as a function of θ until the source is limited at the detector by the slit system. In order to evaluate the geometry factor over the whole length of effective target, it is necessary to do a numerical integration from the point where the element of target no longer sees all of the detector to the point where the detector is completely hidden behind the slit system. The uranium slits are not perfectly opaque to the mesons, therefore, geometrical considerations based on the opaque slit must be corrected.

VI. CORRECTIONS

In order to obtain the proper values of the cross sections, certain corrections must be applied to the data which are inserted into the cross section formulae.

A. Decay in Flight

As the time of transit of the meson, in its own frame, from the source to the detectors is not negligible compared to its mean life of 2.6×10^{-8} sec.,[27,28] a small fraction of the π^- and π^+ mesons will decay before reaching the detector. The evidence is now fairly good that both π^+ and π^- mesons have the same mean life;[41] therefore, the fraction which decay is the same in either case. The correction that was applied to the data is shown in Fig. 15. The correction is small -- ranging from 5 percent at low energies to 2.5 percent at high; therefore, even if the π^- and π^+ mean lives differ slightly this will

have very little effect on the results.

This correction should not be applied to the π-β coincidence crystal detection. In this method of detection, the decay μ mesons may open the time gate in place of the original π meson. The velocity of the μ meson, which always corresponds to an energy of ejection of about 6 Mev in the π meson frame, is usually small in comparison with the π meson velocity so that the trajectory is very close to the one which would have been taken by the π meson. If one neglects the different range-energy relationship for the μ mesons, the density of mesons in the detector should equal that expected for the π mesons had they not decayed. In the case of bombardment of hydrogen one should, therefore, apply no correction. However, in the case of the bombardment of deuterium, additional gates are opened by the μ^- mesons from the decay of the π^- mesons. Thus, too many gates are opened and one should subtract this number from the total to get the true number of π^+ mesons that were emitted from the target.

B. Slit Penetration

The geometry factor, $G(\bar{\theta})$, was calculated on the basis of perfectly opaque slits to the π mesons. This is obviously an oversimplification as some mesons of high energy may penetrate the slit and still have enough energy to reach the detectors; these mesons will then be observed at a lower meson energy. It is clear that this effect will be negligible if the slit aperature is very wide, but quite large if it is narrow. One of the design requirements, therefore, was a wide aperture. The second requirement was a very high density material for the slit system in order to degrade the meson energy in a short length of path.

For the calculation of the correction, a rectangular energy distribution was assumed which gives an approximate fit to the observed spectrum. A given meson detection energy, E, is considered; into its energy interval dE will come mesons from all higher energies which pass through a thickness of the slit sufficient to degrade their energies the proper amount. By assuming the square spectrum a great simplification in calculation occurs, because then the same number of mesons come into the dE interval from each of the other energies. The problem can now be treated as an increase in solid angle which occurs by removing a portion of the slit to the line drawn along the trajectory of the highest energy meson. This process was repeated for several different energies and the curves of Fig. 15 were drawn. This calculation could be made considering the details of the spectrum; however, the correction was at most about 15 percent at the lowest energies in the 45° spectrum, and this calculation would involve only a second order correction to the one from the rectangular distribution.

C. Multiple Scattering

A consideration in the design of the collimation system was to prevent electrons and mesons from scattering off the edges of the slit system into the nuclear emulsions or the crystal detectors. In the case of the emulsions, this was accomplished by scanning only the area of the emulsion that was in the shadow of the straight edge of the slit. This was nearly accomplished in the case of the crystals, also, as only a small fraction of the volume of the crystal in which the mesons stopped protruded out of the shadow.

For the emulsion detection the condition for "poor geometry" was satisfied. The front edge of the emulsion was in contact with the lead

absorber and the thickness of the emulsion, about 2×10^{-2} cm, was very small compared to the height of the lead absorber, 4.5 cm. In the plane of the emulsion the absorber may be considered almost of infinite extent. The r.m.s. displacements for π mesons due to multiple scattering in the different lead absorbers and 1.27 cm of glass were calculated.[21,22] For low energy mesons of 40 Mev the r.m.s. displacement was found to be 0.4 cm. For the high energy mesons of 150 Mev it was 2.1 cm. As the half-width of the absorber was 2.25 cm the net loss of π mesons to the detector is negligible.

For the crystal coincidence detection the poor geometry condition was not entirely satisfied. The reasons for this were: 1) the center of the final crystal was about 4.4 cm from the back edge of the lead absorber. 2) Although the lead absorbers had almost infinite extent in the plane of the collimator, they were only slightly larger than the crystals in the direction perpendicular to this plane.

In order to calculate the fraction of mesons which were lost to the detector by multiple scattering, the distribution function of Eyges[21] and the calculations of Foldy[22] were used. This function was then numerically integrated through the absorber in the direction perpendicular to the plane of the collimating system for various points on the detector and for various initial meson energies. The resulting correction factors for the data are shown in Fig. 15.

D. Nuclear Interactions in Absorbers

The π mesons in traversing matter may interact with the nuclei. Because these mesons may be absorbed, or may undergo large angle scattering, they will not reach the detector. Furthermore, even if the "poor geometry" condition is satisfied for large angle scattering, the

mesons scattered at large angles will be so reduced in energy by the time they reach the detector that they will be observed at an energy lower than those which did not undergo the large scattering. At the present time, the evidence is fairly good that the cross section for these nuclear events for π mesons in flight traversing matter is of the order of a geometrical nuclear area.[42,43,44] The values of nuclear areas found from high energy neutron scattering experiments were used in obtaining this correction factor.[45,46] This correction varies from about 8 percent at a π meson energy of 35 Mev to 85 percent at 150 Mev. Wherever this correction has been applied to the data, it has been indicated by a dotted line.

E. Line Source

The source of π mesons has been treated as a line source. This is a good approximation as the spread of the photon beam at the target, 0.56 inch to 0.71 inch, was small compared to the distance of the center line of the target to the center of the detector, 9.2 inches. In addition, the intensity of the photon beam falls to less than half intensity at 0.5 inch from its center. Solid angle calculations made by integrating over the whole volume of target bombarded by the photons should differ by less than 1 percent from those made for the line source.

F. Photon and Meson Energy Loss in the Target

The photon beam traversed 0.85 gram per cm^2 of stainless steel in the end of the target and 1.9 gram per cm^2 of deuterium from the front to the rear of the target. The photon beam is attenuated by less than 4 percent in the target end wall and by less than 2 percent in the 24 inches of path length in deuterium or hydrogen. The 4 percent loss is

negligible compared to the absolute error in beam monitoring. The 2 percent loss over the entire length of the target that might affect relative values between the 135° angle and 45° is considerably less than the statistics, and of the same order of accuracy as the relative beam monitoring.

The energy loss of π mesons in the gas of the target is less than one Mev for all but the lowest energy mesons. This gives a maximum uncertainty to the meson energy, due to target, of less than 2 Mev. This is small compared to the detector energy widths which range from 5 to 20 Mev.

VII. RESULTS

A. Minus-Plus Ratio for Deuterium

The values for the ratio of the number of π^- to π^+ mesons observed at an angle of emission of 45° are plotted in Fig. 15 as a function of the π meson energy. The mean of the values at 45°, 90°, and the mean of all of the data are given in Table V. The errors given in Table V and the following tables are standard deviations due to statistics, only.

Table V. Mean minus-plus ratios from deuterium

Angle $\bar{\theta}$	Mean energy (Mev)	Experimental Ratio	Experimental Ratio (Alternate Method)
45°	61	0.96 ± 0.11	0.98 ± 0.13
90°	70	0.98 ± 0.14	1.08 ± 0.19
45° and 90°		0.97 ± 0.09	1.01 ± 0.12

If systematic errors in the plate reading exist, they would tend to lower this ratio slightly. These ratios show no variation within statistics with the energy or angle of emission of the π mesons. That

the ratio is close to one is in agreement with the results of Littauer and Walker[7] who found a value of 1.19 ± 0.12 for a meson energy of 50 Mev and angle of emission of 135°.

B. Energy Distributions from Hydrogen and Deuterium at 135°, 90° and 45°

The energy distributions for π mesons from hydrogen and deuterium were calculated in cm^2, per Mev, per steradian per equivalent quantum, per proton as indicated in Section V. Corrections have been made for decay in flight, slit penetration and multiple scattering. The results are plotted in Figs. 17 and 18 for the energy distributions of π^+ mesons at 135° and 90° respectively. On each of these figures appears separately the energy distribution obtained by π-μ, π-β and π-μ-β detection. The combined data is also plotted. In Fig. 19 is plotted the energy distribution for π^+ and π^- mesons at 45°. Smooth curves have been drawn through the combined data points and extrapolated to zero for purposes of integration. These same curves were superimposed upon the data from the separate detection methods for the purpose of intercomparison. Wherever a point appears for π^- data, the cross section is understood to be per neutron in the target instead of per proton.

The absolute cross section scale was fixed by emulsion detection data from hydrogen and deuterium. The relative values of the hydrogen to deuterium energy distributions, at 90° and 135° as obtained by crystal detection, were not altered by this emulsion normalization. The tails on the energy distributions, which appear at meson energies above that allowed by conservation of energy and momentum at the angle, $\bar{\theta}$, are due to those mesons which are allowed through the collimating system at smaller angles than $\bar{\theta}$. The shape of the spectrum at 90° compares favorably with that of previous experimenters[11,12] when the tail, due

to mesons from smaller angles, is taken into account. The absolute value of the peak of the spectrum agrees with that of Bishop[47] for π^+ mesons from liquid hydrogen but is 1.5 times the published value.[11,12] The energy spectrum for hydrogen lies above that for deuterium at each of the angles of 45°, 90° and 135°. The combined data are plotted in Fig. 20 for each of the angles along with curves that are corrected for nuclear absorption.

The relative photon beam integration for the experiment is considered to be good to 2 percent. However, the uncertainty in absolute integration might be as large as 20 percent. The absolute values also have an uncertainty of 5 percent which comes from the absolute measurements of emulsion thicknesses. The relative uncertainties of plate thicknesses are only about 2 percent. These uncertainties are present, also, in the following results.

C. Differential Cross Sections

The areas under the curves of Fig. 20 were found by numerical integration. The values obtained for π^+ mesons are given in Table VI. These would be changed somewhat by a different extrapolation to zero energy. The errors given are standard deviations based only on the statistics of the energy regions covered by the experiment. The value at 45° relative to the values at 90° and 135° are only as good as the statistics of the emulsion normalization, about 10 percent.

The values of Table VI are plotted in Fig. 21. Smooth curves were drawn through the points for the purpose of integration. The curves which include the correction for nuclear interactions is also plotted.

Table VI. Differential cross sections for π^+ mesons from deuterium and hydrogen

Target	$\bar{\theta}$	$\frac{d\sigma(\bar{\theta})}{d\Omega}$ cm^2 (steradian)$^{-1}$ (equivalent quantum)$^{-1}$ (proton)$^{-1}$	$\left(\frac{d\sigma(\bar{\theta})}{d\Omega}\right)$ corrected Corrected for Nuclear Absorption
Deuterium	135°	$4.3 \pm 0.3 \times 10^{-30}$	$4.8 \pm 0.3 \times 10^{-30}$
	90°	5.5 ± 0.3	6.7 ± 0.4
	45°	4.5 ± 0.4	5.5 ± 0.5
Hydrogen	135°	5.4 ± 0.2	6.0 ± 0.2
	90°	7.4 ± 0.3	9.1 ± 0.3
	45°	5.5 ± 0.4	7.1 ± 0.5

D. Total Cross Sections

The total cross sections for π^+ mesons from hydrogen and deuterium were found by integrating the differential cross sections of Fig. 21 over the solid angle. In addition to the uncertainties listed previously there is the uncertainty due to the extrapolation over angles for which the differential cross sections were not obtained. Since the solid angle approaches zero at 0° and 180°, and since the differential cross sections apparently drop at large and small angles, this extrapolation introduces a smaller error than it otherwise would. The total cross sections are given in Table VII.

Table VII. Total cross sections for π^+ mesons from deuterium and hydrogen

Target	$\bar{\sigma}_T$ cm^2 (equivalent quantum)$^{-1}$ (proton)$^{-1}$	$\bar{\sigma}_T$ corrected Corrected for Nuclear Absorption
Deuterium	$6.1 \pm 0.3 \times 10^{-29}$	$7.7 \pm 0.3 \times 10^{-29}$
Hydrogen	7.8 ± 0.2	9.5 ± 0.3

E. Ratios of Cross Sections of Deuterium to Hydrogen

The ratios of the cross sections for the production of π^+ mesons from deuterium and hydrogen in cm^2 per Mev, per steradian, per equivalent quantum, per proton have been calculated for several energies at each of the three angles, 45°, 90° and 135°. These values are plotted in Fig. 22. The ratios at 135° and 90° are dependent only on relative counting efficiencies, relative beam monitoring, and number of target protons per cm^3 that were bombarded, and are therefore independent of the absolute beam monitoring. The ratio at 45° has, in addition, the uncertainty of 2 percent in relative plate thicknesses. For these ratios, therefore, the largest uncertainties are given by the statistics.

At each of the three angles, it is fairly certain that the ratios are less than one. The statistics are not good enough to establish a dependence on energy. At 90° where both emulsion and counter data were obtained, it is gratifying that the ratios agree. At a meson energy of 50 Mev and angle of emission of 135°, Littauer and Walker[7] found a ratio of 0.87 ± 0.08. The corresponding value in Fig. 21 is in good agreement with this.

The ratios of the differential cross sections for π^+ meson production are given in Table VIII. The ratios there and in Fig. 23 have not been corrected for nuclear interaction. If nuclear interaction were included, the 135° and 90° ratios would remain unchanged, but the 45° ratio would be increased by 4 percent. These ratios are dependent on the relative shapes of the energy distributions in the extrapolated energy regions where data was not obtained. As the hydrogen and deuterium energy distributions appear to have about the same shape the error introduced in the extrapolated regions is probably not large.

The experimental value of the ratio of the total cross sections is

Table VIII. Ratios of differential cross sections for π^+ mesons from deuterium and hydrogen

Angle ($\bar{\theta}$)	$\frac{\left(\frac{d\sigma(\bar{\theta})}{d\Omega}\right)_D}{\left(\frac{d\sigma(\bar{\theta})}{d\Omega}\right)_H}$
45°	0.81 ± 0.10
90°	0.75 ± 0.05
135°	0.80 ± 0.06

0.78 ± 0.03. In this case the value is dependent on the relative shapes of the energy spectra at angles which were not measured and the assumption of similar shapes of the spectra become suspect. Systematic errors due to this could cause uncertainties larger than the statistical uncertainty.

VIII. CONCLUSIONS

The evidence presented in the preceding section seems fairly positive that the minus-plus ratio from deuterium is close to one and that it is relatively insensitive to the meson energy or angle of emission. As the deuteron consists of a loosely bound neutron and proton, it is difficult to see how nuclear structure can affect this ratio to any extent, either in changing the free nucleon-meson interaction or in absorption or other interactions of the π mesons before leaving the nucleus. If the neutron then acts as a free particle, except for the small binding energy and the exclusion principle effects, the photomeson production process must be essentially independent of the charge carried by the nucleon, other than determining the sign of the meson produced.

Theoretical calculations by Brueckner,[9] based on the currents due

to the charges of the moving protons and mesons, yield minus-plus values which are greater than one and show angle and energy dependence. However, when he used an interaction of the photon with the anomalous magnetic moments of the nucleons, he obtained minus-plus ratios that were essentially one, independent of angle and energy. This suggests that the photon interaction with moving charges is not sufficient to explain the ratio and that the photon interaction with the magnetic moments of the nucleons is important in the production process.

Meson theories, in general, have not been successful in explaining either nuclear forces or meson production. The pseudo-scalar theory has, in some instances, given reasonable qualitative agreement with theory, but has not been capable of making quantitative prediction.

The phenomenological approach which has recently been taken by several investigators, although less fundamental to the problem of meson-nucleon interactions, seems capable of making quantitative predictions. Of special interest is the theoretical work of Chew and Lewis[17] on the production of photomesons from deuterium.

They have considered the reaction for photomeson production from a free proton

$$k_o + H \longrightarrow n + \pi^+$$

and from a deuteron

$$k_o + D \longrightarrow 2n + \pi^+$$
$$\longrightarrow 2p + \pi^-$$
$$^3S \qquad ^1S,\ ^3P \ldots$$

The deuteron is initially in the ^3S state (96 percent). As the final state of the two neutrons must be antisymmetric, they can be only in the ^1S, ^3P,..... states. Unless the proton in the deuteron flips its spin in the reaction, the available phase space is reduced

and the cross section is down relative to the cross section for production from a free proton.

In addition to the reduction because of the exclusion effects, the cross section will be reduced because of the binding in the deuteron.

For the case of the bombardment of a free proton by a photon of energy, k_o, at an angle of emission, θ, the meson energy, E_π^o is specified by conservation of energy and momentum. In the case of bombardment of a deuteron, the meson energy is no longer specified but will have a spectrum with its most probable value at E_π^o. Chew and Lewis find that the ratio of the cross sections of deuterium to hydrogen, for a particular k_o and θ, is of the form

$$\frac{d\sigma(\theta,k_o)_D}{d\sigma(\theta,k_o)_H} = \frac{a(\theta,k_o)\ |f_o|^2 + b(\theta,k_o)\,|f_1|^2}{|f_o|^2 + |f_1|^2}$$

where f_o is the amplitude for non-spin flip of the proton and f_1 is the amplitude for spin flip. By an accurate measurement of the ratio of the cross sections the experimenter could determine $\frac{|f_1|^2}{|f_o|^2 + |f_1|^2}$, the fraction of protons that flip their spins. Since the pseudoscalar meson theory involves a spin interaction, a measurement of the spin flip probability could be used as a check on the theory.

Monochromatic photon beams of sufficient energy for meson production are not available. However, if the deuteron spectrum is quite sharp the photons of an energy not equal to k_o in the bremsstrahlung beam will not contribute appreciably to the number of mesons at a particular angle, θ, and energy of the meson, E_π, and the above equation should apply.

In one method used by Chew and Lewis for calculating a and b, the final state of the two neutrons must be specified. Plane waves for the

outgoing neutrons were chosen in order to simplify the calculations although there will be some interaction in the "dineutron." This neglect of the "scattering" of the two neutrons tends to underestimate slightly the ratio of the cross sections.

Another method, suggested by Chew and Lewis for evaluating a and b, makes use of the closure principle in such a way that the wave functions of the final neutrons can remain unspecified. This method tends to overestimate the ratio slightly.

In order to have a large exlusion effect, the relative momentum of the two outgoing neutrons must be small. Unfortunately, this occurs at small angles to the photon beam direction where the background due to electrons is very high. At angles where the exclusion effect is large, the deuterium spectrum is also sharp and the bremsstrahlung beam should not present a problem.

The functional form of a and b has been evaluated by the above authors by the first method and a and b have been computed for a few cases. These ratios appear in Table IX. Although the deuterium spectrum at 90° is probably not sharp, and, therefore, the computations may not be applicable, they have been included in Table IX.

Table IX. Values of "a" and "b" for deuterium-hydrogen ratio

θ	k_o (Mev)	E_π (Mev)	a	b
90°	211	40	0.64	0.76
	260	70	0.76	0.84
45°	192	40	0.56	0.79
	227	70	0.66	0.91

It is at once apparent, if one compares the spread in the theoretical values with the experimental statistics, that the data is not accurate enough to distinguish between flip and non-flip at either 90°

or 45°. However, there is qualitative agreement between theory and experiment. The agreement is close enough that one is encouraged either to obtain considerably more data at 45° or to attempt to measure the ratio at a much smaller angle to the photon beam where the difference in the theoretical values for spin flip and non-spin flip is greater and therefore the statistics needed are less.

IX. ACKNOWLEDGMENTS

I wish to express my appreciation to Professor E. M. McMillan for his continued guidance and support. I am indebted to Mr. M. J. Jakobson and Mr. A. G. Schulz for their cooperation and assistance throughout the course of the experiment. I would like to thank Professors W. K. H. Panofsky and O. Chamberlain for much helpful discussion. I am indebted to Dr. R. L. Aamodt and Professor W. K. H. Panofsky for use of their deuterium pumping system, to Professors G. F. Chew and H. W. Lewis for a pre-publication copy of their paper on photomeson production from deuterons and to Mr. H. Savage for numerical evaluation of the theoretical ratio that appears therein. I wish to thank Dr. W. H. Barkas and other members of the Film Group for the use of their facilities, and Mr. E. Bailey for assistance in compiling the thesis. My sincere thanks go to Mr. George McFarland and other members of the synchrotron crew for help in making the bombardments.

I wish to dedicate this thesis to my wife, Freda, for her constant encouragement throughout this work.

X. REFERENCES

1. Lattes, Muirhead, Occhialini and Powell, Nature 159, 694 (1947)
2. E. Gardner and C. M. G. Lattes, Science 107, 270 (1948)
3. E. M. McMillan and J. M. Peterson, Science 109, 438 (1949)
4. McMillan, Peterson and White, Science 110, 579 (1949)
5. Peterson, Gilbert and White, Phys. Rev. 81, 1003 (1950)
6. McMillan, Blocker and Kenney, Phys. Rev. 81, 455 (1951)
7. R. M. Littauer and D. Walker, Private Communication
8. Camac, Corson, Littauer, Shapiro, Silverman, Wilson, and Woodword, Bull. Am. Phys. Soc. 26, (1), 48 (1951)
9. K. A. Brueckner, Phys. Rev. 79, 641 (1950)
10. ~~L. J. Cook, Private Communication~~
11. J. Steinberger and A. S. Bishop, Phys. Rev. 78, 494 (1950)
12. Bishop, Steinberger and Cook, Phys. Rev. 80, 291 (1950)
13. R. F. Mozley, Phys. Rev. 80, 493 (1950)
14. H. A. Medicus, Bull. Am. Phys. Soc. 26 (3), 15 (1951)
15. M. J. Jakobson, Ph. D. Thesis, Univ. of California (1951)
16. H. Feshbach and M. Lax, Phys. Rev. 76, 134 (1949)
17. G. Chew and H. Lewis, Pre-publication Paper
18. R. F. Mozley and R. S. White, Private Communication
19. Panofsky, Aamodt and Hadley, Phys. Rev. 81, 565 (1951)
20. Johnston, Bezman, Rubin, Swanson, Corak and Rifkin, MDDC-850
21. L. Eyges, Phys. Rev. 74, 1535 (1948)
22. L. L. Foldy, Phys. Rev. 75, 311 (1949)
23. Aron, Hoffman and Williams, UCRL-121, 2nd Rev. (1949)
24. W. A. Aron, Private Communication
25. Bradner, Smith, Barkas and Bishop, Phys. Rev. 77, 462 (1950)
26. Univ. of California Radiation Laboratory Film Group, Private Communication

27. Chamberlain, Mozley, Steinberger and Wiegand, Phys. Rev. 79, 394 (1950)

28. Jakobson, Schulz and Steinberger, Phys. Rev. 81, 894 (1951)

29. Alvarez, Longacre, Ogren and Thomas, Phys. Rev. 77, 752 (1950)

30. C. Wiegand, Rev. Sci. Inst. 21, 975 (1950)

31. F. M. Smith, Phys. Rev. 81, 897 (1951)

32. H. L. Friedman and J. Rainwater, Phys. Rev. 81, 644 (1951)

33. F. L. Adelman and S. B. Jones, Science 111, 226 (1950)

34. Leighton, Anderson and Seriff, Phys. Rev. 75, 1432 (1949)

35. S. B. Jones and R. S. White, Phys. Rev. 82, 374 (1951)

36. E. P. George and J. Evans, Proc. Phys. Soc. (London) 64 (2), 193 (1951)

37. Blocker, Kenney and Panofsky, Phys. Rev. 79, 419 (1950)

38. Jakobson, Private Communication

39. Cartwright, Richman, Whitehead and Wilcox, Phys. Rev. 81, 652 (1951)

40. F. L. Adelman, Ph. D. Thesis, Univ. of California, UCRL-1005

41. Lederman, Tinlot and Booth, Phys. Rev. 81, 281 (1951)

42. Chedister, Isaacs, Sachs and Steinberger, Pre-publication Paper

43. H. Bradner and B. Rankin, Phys. Rev. 80, 916 (1950)

44. Bernardini, Booth, Lederman and Tinlot, Phys. Rev. 80, 924 (1950)

45. Cook, McMillan, Peterson and Sewell, Phys. Rev. 75, 7 (1949)

46. Fernbach, Serber and Taylor, Phys. Rev. 75, 1352 (1949)

47. A. S. Bishop, Ph. D. Thesis, Univ. of California, UCRL-874 (1950)

48. G. Gauer and C. Nunan, UCRL-714 (1950)

1/2 life π Richardson PR 74 1726
Panofsky PR 77 454

XI. ILLUSTRATIONS

Fig. 1. Schematic layout of the essential experimental components.

Fig. 2. Photograph of the experimental equipment showing the gas target, collimating system, detectors, and gas pumping system.

Fig. 3. Assembly of the gas target.

Fig. 4. Schematic drawing of the gas pumping system.

Fig. 5. Photograph of a close-up view of the gas target, collimating system, and detectors.

Fig. 6. Schematic drawing of a vertical section through the target and the collimating system, with the detectors in position.

Fig. 7. Schematic drawing of a horizontal section through the target and the collimating system with the detectors in position.

Fig. 8. Plot of the angular distribution of π^+ and σ mesons for the 45° and 90° collimating systems demonstrating the angular resolution. The mesons have a mean energy of 70 Mev. The angles were measured at 200 microns back from their endings. The dotted line represents the calculated resolution neglecting multiple scattering. The heavy black lines are located at the r.m.s. angle of the distribution if multiple scattering is included.

Fig. 9. Block diagram of the electronics used in the crystal coincidence detection.

Fig. 10. Depth distribution of π-μ, σ, ρ and μ^+ meson endings.

Fig. 11. Projected track length distribution of π-μ, σ, ρ and μ^+ mesons. The track lengths were measured from their endings, back to the point where they entered or left the emulsion. The track lengths were measured to only 10 percent accuracy. The curve on the μ^+ meson range distribution plot is the expected distri-

bution based on normalization between 50 and 500 micron ranges.

Fig. 12. Distribution in angle of the π-μ, σ, ρ and μ^+ mesons from deuterium for the 45° collimating system. The angles were measured at the point where they entered the emulsion, or 200 microns back from their ending, whichever was the shorter. The abscissa is the angle to the beam direction.

Fig. 13. Distribution in angle of the π-μ, ρ, and μ^+ mesons from hydrogen for the 45° collimating system. The angles were measured at the point where they entered the emulsion, or 200 microns back from their ending, whichever was the shorter. The abscissa is the angle to the beam direction.

Fig. 14. Schematic drawing of the line source and detector element.

Fig. 15. Curves showing the correction factors applied to the data for time of flight, slit penetration, and multiple scattering. These are given for the coincidence crystal detection at 90° and 135°, and for the emulsion detection at 45° and 90°. No correction for multiple scattering was necessary in the case of emulsion detection.

Fig. 16. Plot of the minus-plus ratio for deuterium versus the meson energy at 45°. One point is included for 90°.

Fig. 17. Energy distributions at 135° to the beam direction for π^+ mesons from deuterium and hydrogen. Separate plots are shown for π-μ, π-β, and π-μ-β coincidence crystal detection. The combined data plot is also shown. A smooth curve was drawn on the combined data plot for purposes of integration. This curve was drawn on the other plots for the purpose of intercomparison. The dotted line has been extrapolated into zero energy.

Fig. 18. Energy distributions at 90° to the beam direction for π^+ mesons

from deuterium and hydrogen. Separate plots are shown for π-μ, π-β, and π-μ-β coincidence crystal detection. The combined data plot is also shown. Three points from emulsion detection are plotted. A smooth curve was drawn on the combined data plot for purposes of integration. This curve was drawn on the other plots for the purpose of intercomparison. The dotted line has been extrapolated into zero energy.

Fig. 19. Energy distributions at 45° to the beam direction for π^+ and π^- mesons from deuterium and π^+ mesons from hydrogen. A smooth curve was drawn through the points for the purposes of integration. The dotted line has been extrapolated into zero energy.

Fig. 20. Intercomparison of the data at 135°, 90° and 45° for deuterium and hydrogen respectively. The curves which have been corrected for nuclear interactions in the absorbers have also been included. The cross section for nuclear interactions was taken as one nuclear area.

Fig. 21. Differential cross sections for π^+ mesons from deuterium and hydrogen. Smooth curves were drawn for the purpose of integration and extrapolated into 0° and 180°. The curves which have been corrected for nuclear interactions in the absorbers have also been included. The cross section for nuclear interactions was taken as one nuclear area.

Fig. 22. Ratios of the cross sections (which are given in cm^2 per Mev per steradian per equivalent quantum per proton) for π^+ mesons from deuterium and hydrogen.

Fig. 23. Ratios of the differential cross sections for π^+ mesons from deuterium and hydrogen.

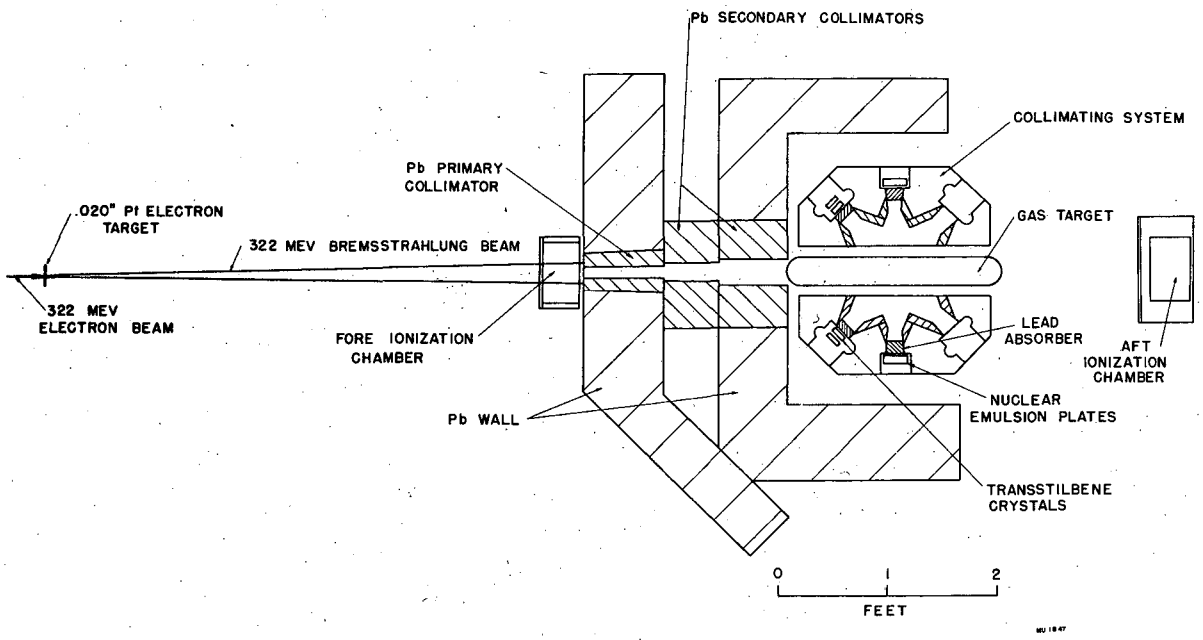
Pb SECONDARY COLLIMATORS
COLLIMATING SYSTEM
Pb PRIMARY COLLIMATOR
.020" Pt ELECTRON TARGET
322 MEV BREMSSTRAHLUNG BEAM
GAS TARGET
322 MEV ELECTRON BEAM
FORE IONIZATION CHAMBER
LEAD ABSORBER
AFT IONIZATION CHAMBER
Pb WALL
NUCLEAR EMULSION PLATES
TRANSSTILBENE CRYSTALS
0
1
2
FEET

Fig. 1

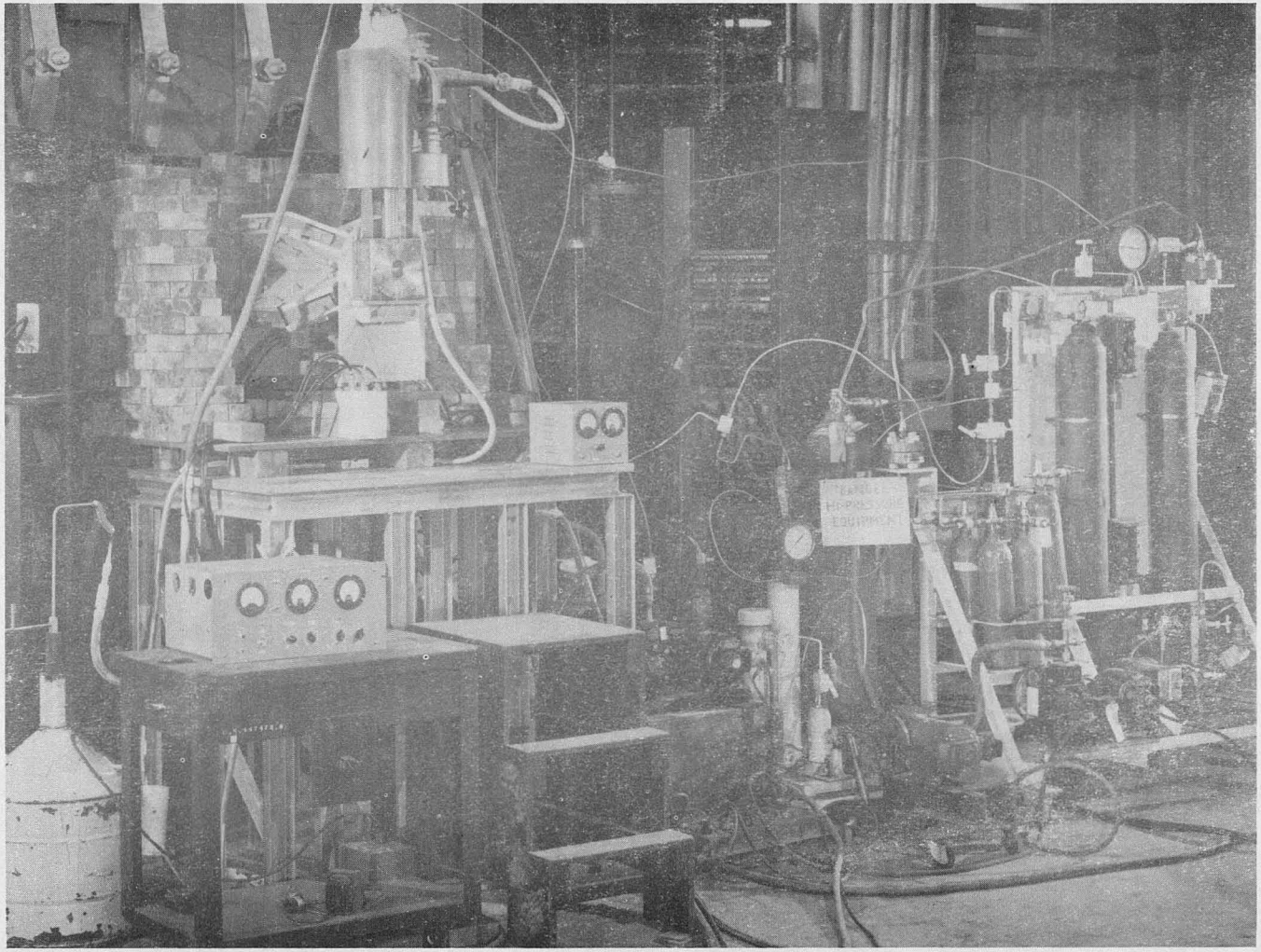

ZN 56

FIG. 2

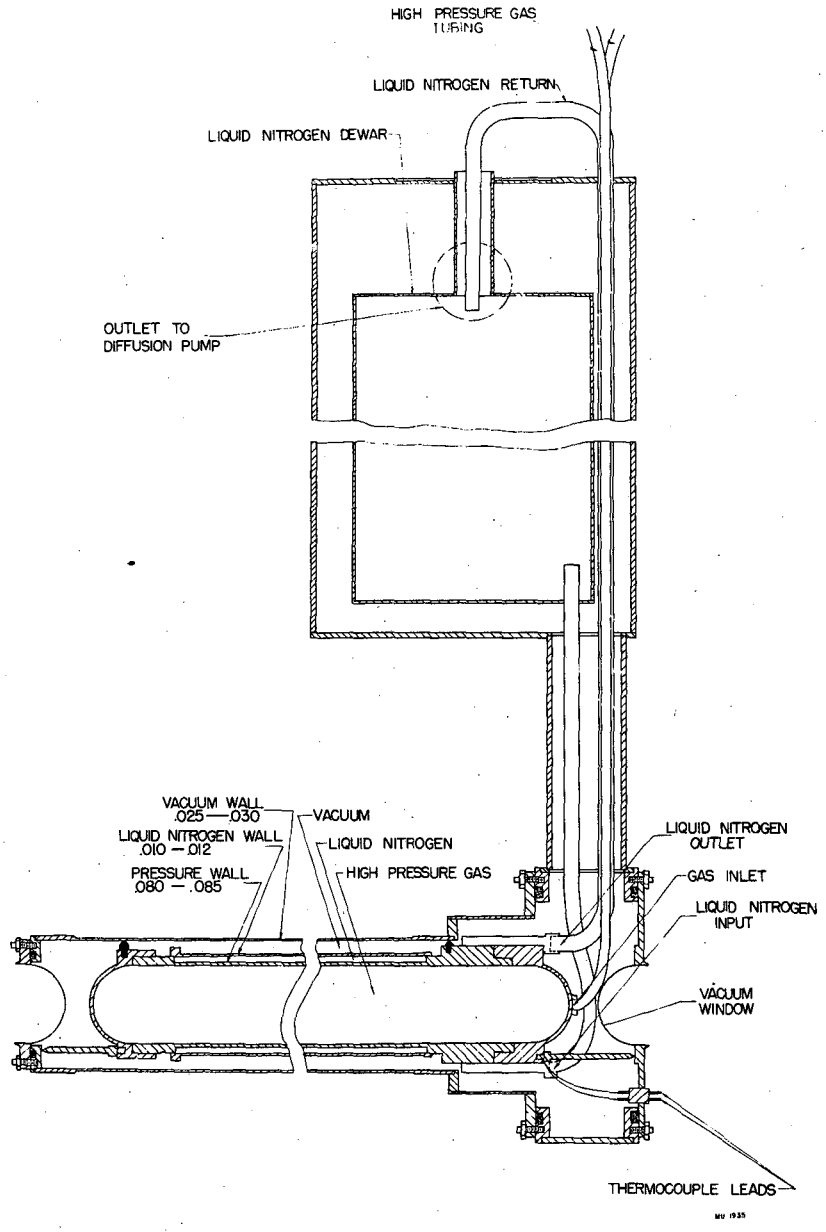
HIGH PRESSURE GAS TUBING
LIQUID NITROGEN RETURN
LIQUID NITROGEN DEWAR
OUTLET TO DIFFUSION PUMP
VACUUM WALL .025—.030
LIQUID NITROGEN WALL .010—.012
PRESSURE WALL .080—.085
VACUUM
LIQUID NITROGEN
HIGH PRESSURE GAS
LIQUID NITROGEN OUTLET
GAS INLET
LIQUID NITROGEN INPUT
VACUUM WINDOW
THERMOCOUPLE LEADS

Fig. 3

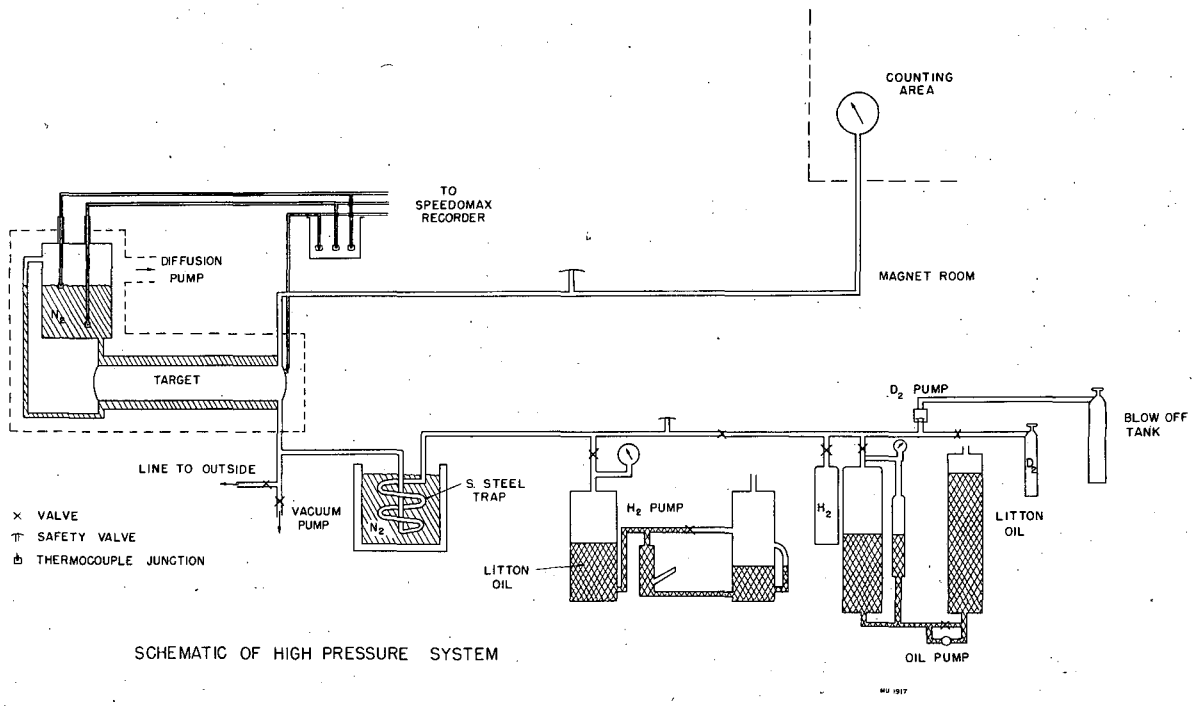

SCHEMATIC OF HIGH PRESSURE SYSTEM

Fig. 4

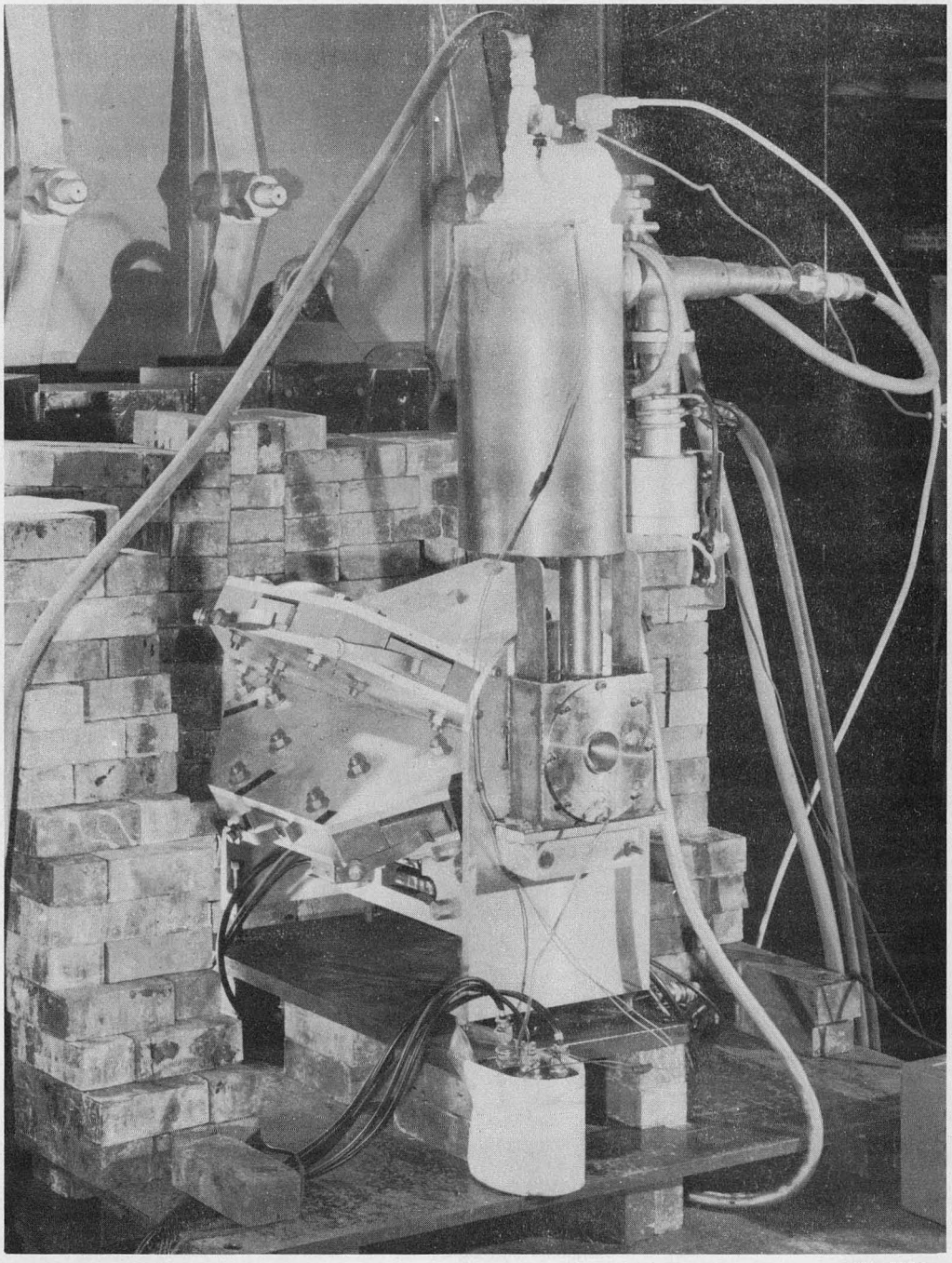

ZN 57

FIG. 5

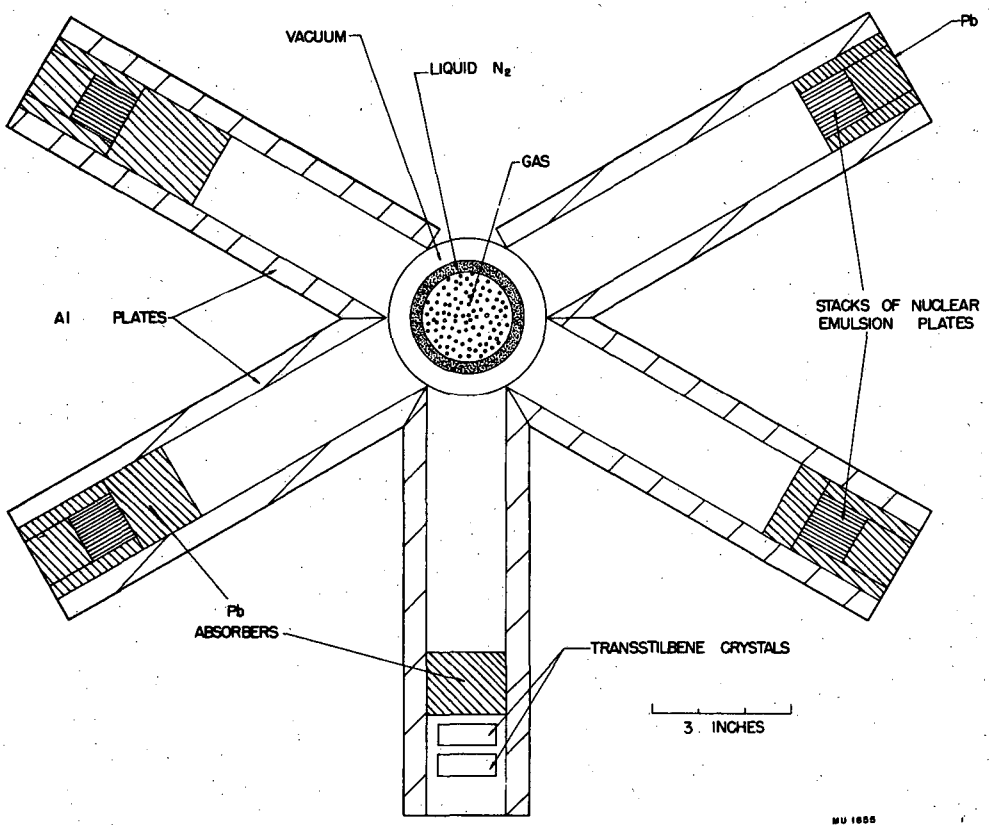
VACUUM
LIQUID N_2
GAS
Pb
Al PLATES
STACKS OF NUCLEAR EMULSION PLATES
Pb ABSORBERS
TRANSSTILBENE CRYSTALS
3 INCHES
MU 1655

Fig. 6

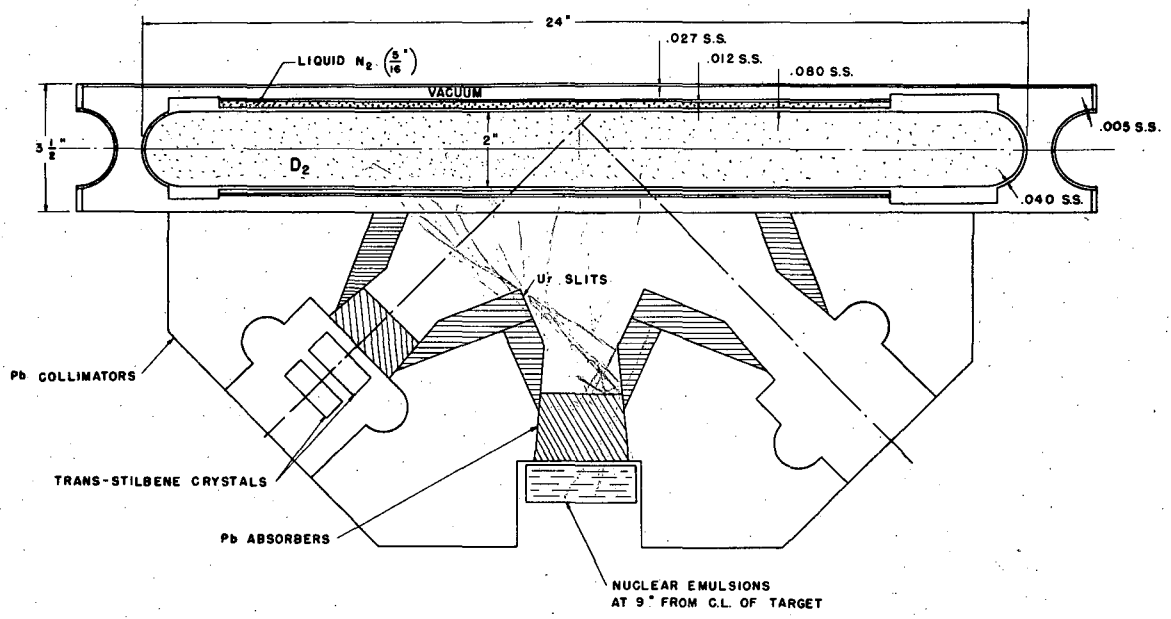
24"
.027 S.S.
.012 S.S.
.080 S.S.
LIQUID N_2 $(\frac{5}{16}")$
VACUUM
$3\frac{1}{2}"$
2"
D_2
.005 S.S.
.040 S.S.
U SLITS
Pb COLLIMATORS
TRANS-STILBENE CRYSTALS
Pb ABSORBERS
NUCLEAR EMULSIONS
AT 9° FROM C.L. OF TARGET
MU 1499

Fig. 7

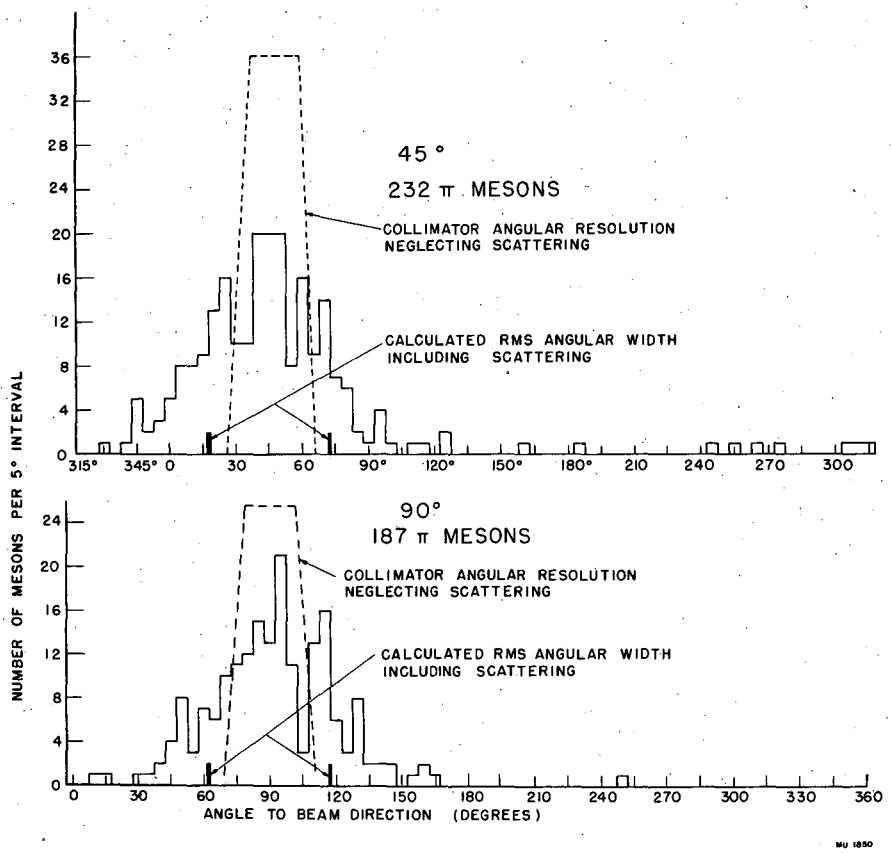
45°
232 π MESONS
COLLIMATOR ANGULAR RESOLUTION
NEGLECTING SCATTERING
CALCULATED RMS ANGULAR WIDTH
INCLUDING SCATTERING
90°
187 π MESONS
COLLIMATOR ANGULAR RESOLUTION
NEGLECTING SCATTERING
CALCULATED RMS ANGULAR WIDTH
INCLUDING SCATTERING
NUMBER OF MESONS PER 5° INTERVAL
ANGLE TO BEAM DIRECTION (DEGREES)
MU 1850

Fig. 8

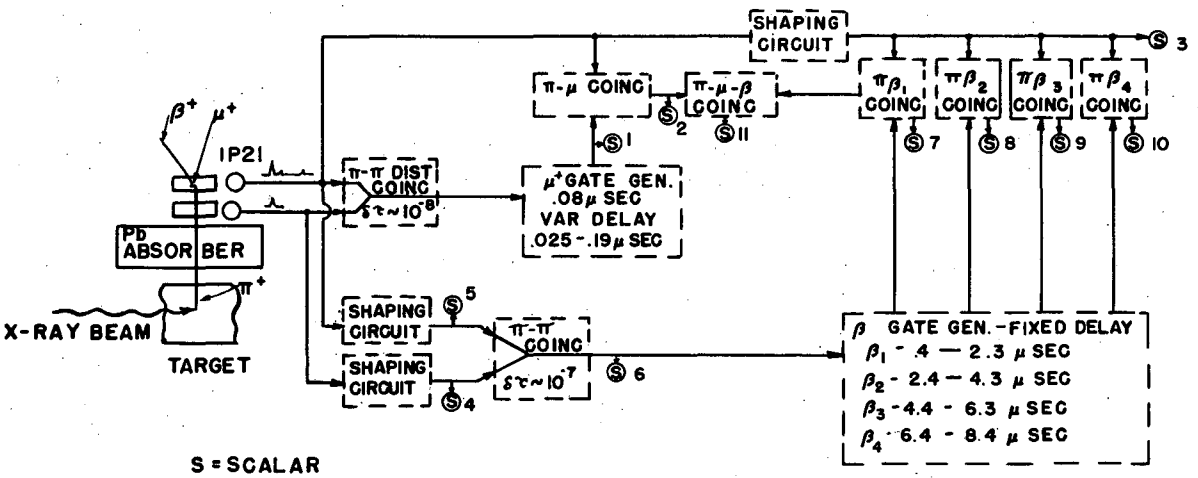

BLOCK DIAGRAM – ELECTRONICS

MU 1864

Fig. 9

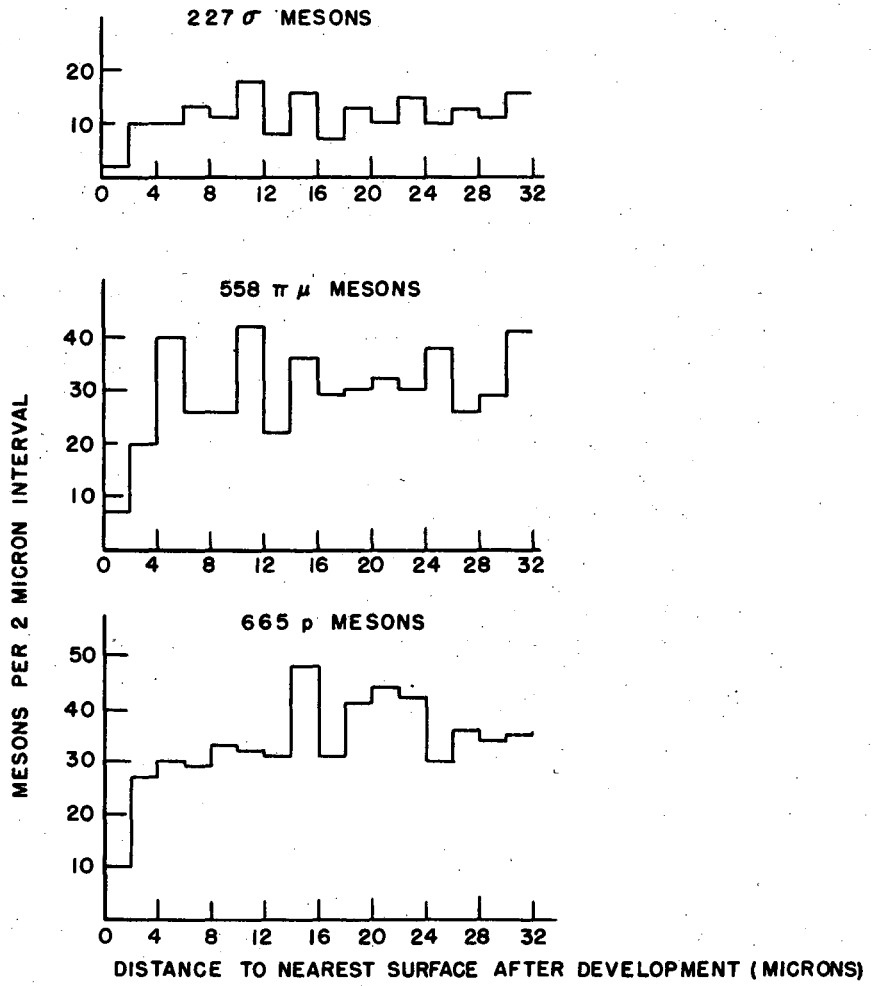
227 σ MESONS
20
10
0 4 8 12 16 20 24 28 32
558 π μ MESONS
40
30
20
10
0 4 8 12 16 20 24 28 32
665 p MESONS
50
40
30
20
10
0 4 8 12 16 20 24 28 32
MESONS PER 2 MICRON INTERVAL
DISTANCE TO NEAREST SURFACE AFTER DEVELOPMENT (MICRONS)
MU 1849

Fig. 10

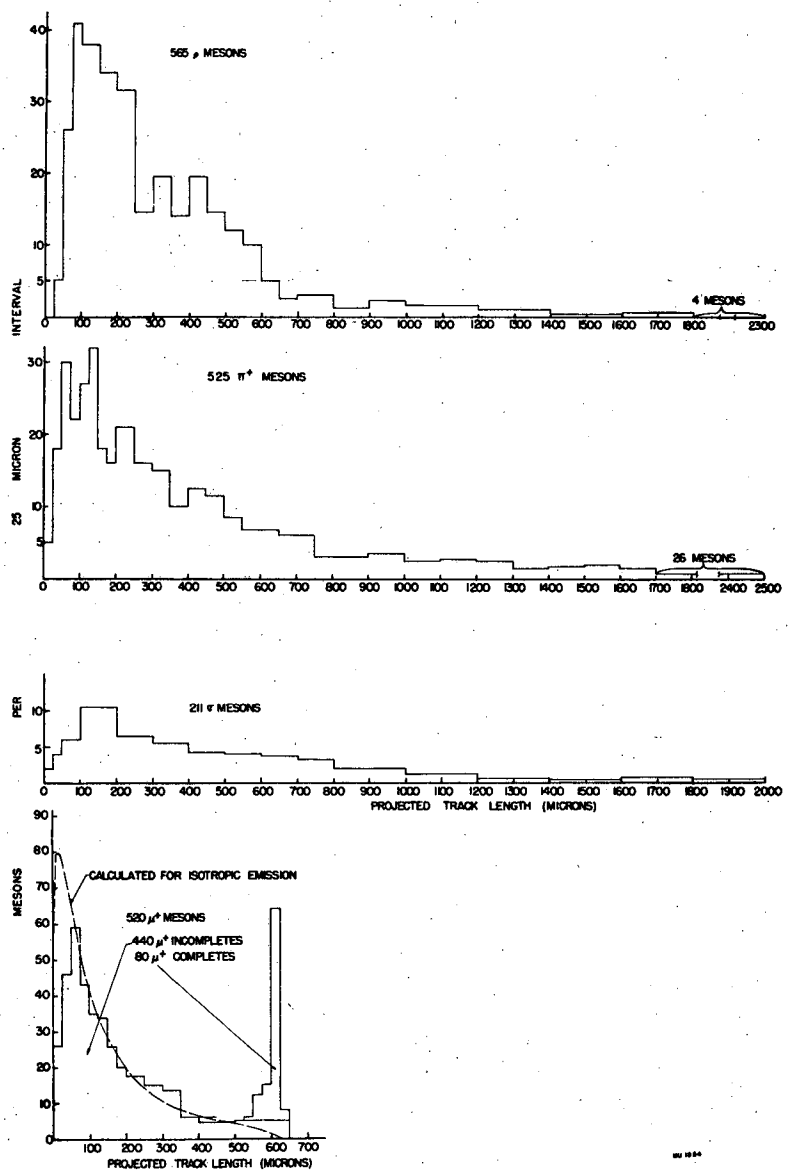
565 ρ MESONS
4 MESONS
INTERVAL
525 π⁺ MESONS
26 MESONS
MICRON
211 σ MESONS
PER
PROJECTED TRACK LENGTH (MICRONS)
CALCULATED FOR ISOTROPIC EMISSION
520 μ⁺ MESONS
440 μ⁺ INCOMPLETES
80 μ⁺ COMPLETES
MESONS
PROJECTED TRACK LENGTH (MICRONS)

Fig. 11

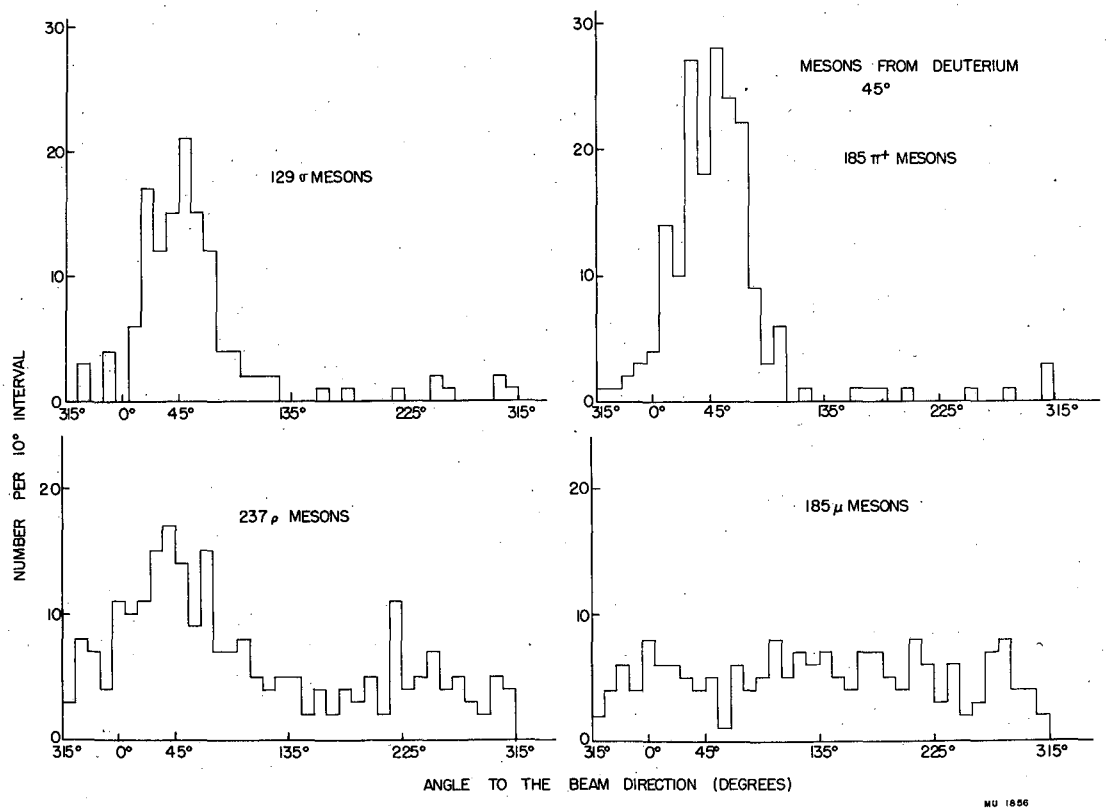
MESONS FROM DEUTERIUM
45°
129 σ MESONS
185 π+ MESONS
237 ρ MESONS
185 μ MESONS
NUMBER PER 10° INTERVAL
ANGLE TO THE BEAM DIRECTION (DEGREES)
MU 1856

Fig. 12

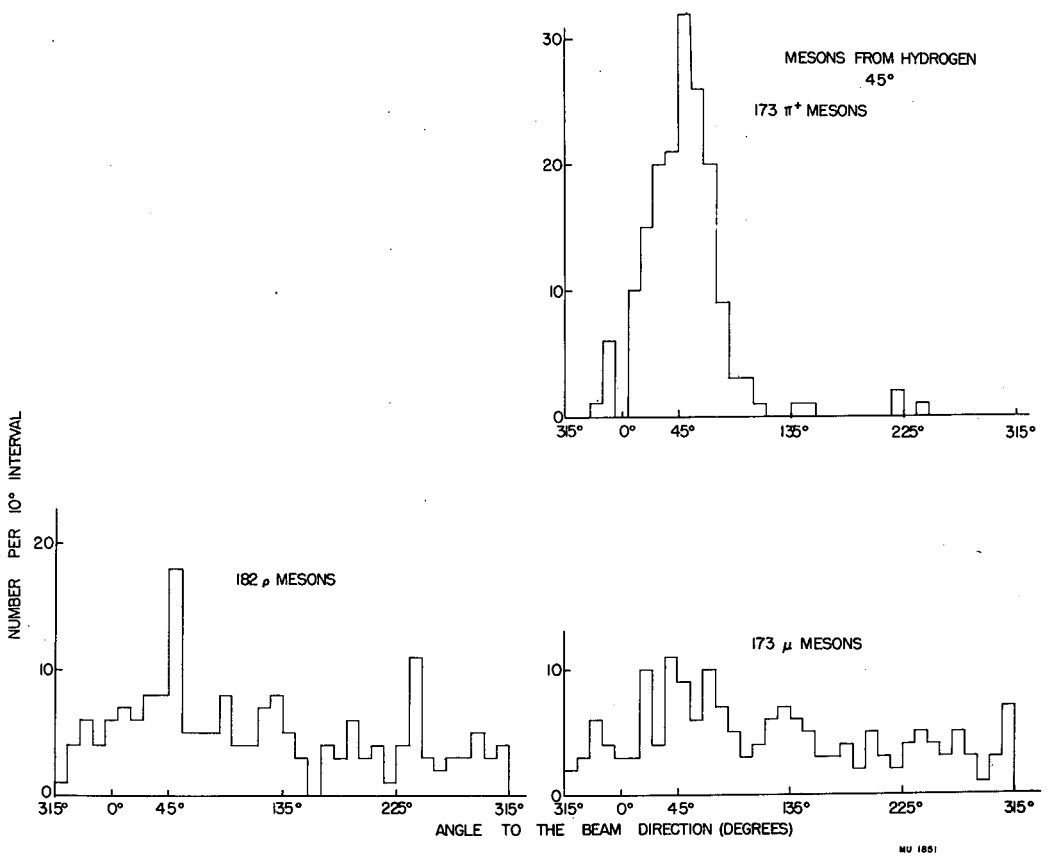
MESONS FROM HYDROGEN
45°
173 π+ MESONS
182 p MESONS
173 μ MESONS
NUMBER PER 10° INTERVAL
ANGLE TO THE BEAM DIRECTION (DEGREES)
315°
0°
45°
135°
225°
MU 1851

Fig. 13

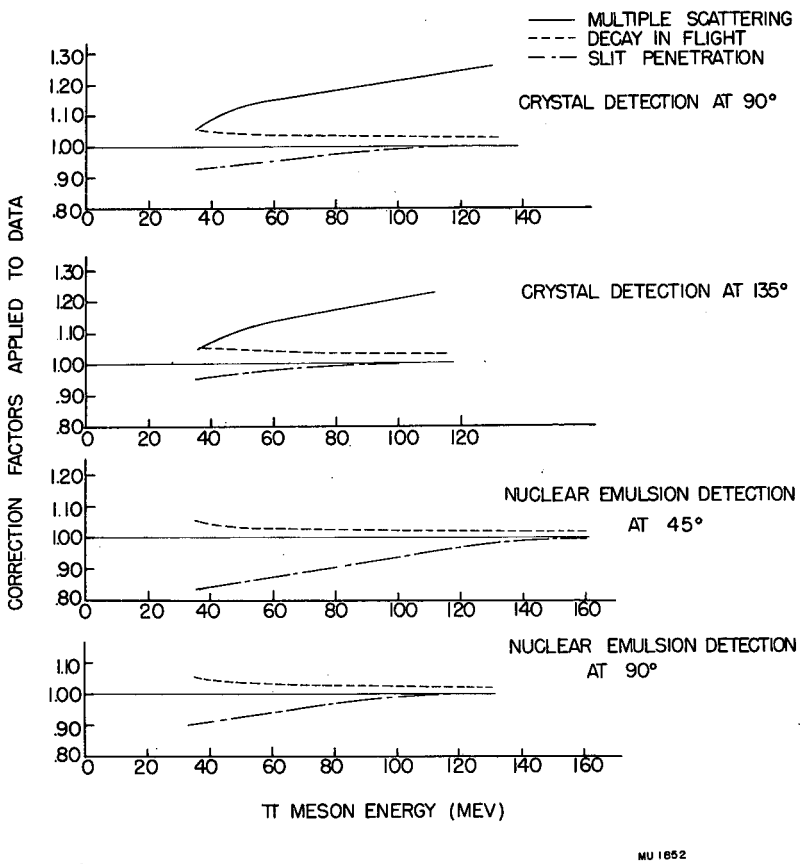
MULTIPLE SCATTERING
DECAY IN FLIGHT
SLIT PENETRATION
CRYSTAL DETECTION AT 90°
CRYSTAL DETECTION AT 135°
NUCLEAR EMULSION DETECTION AT 45°
NUCLEAR EMULSION DETECTION AT 90°
CORRECTION FACTORS APPLIED TO DATA
TT MESON ENERGY (MEV)
MU 1652

Fig. 15

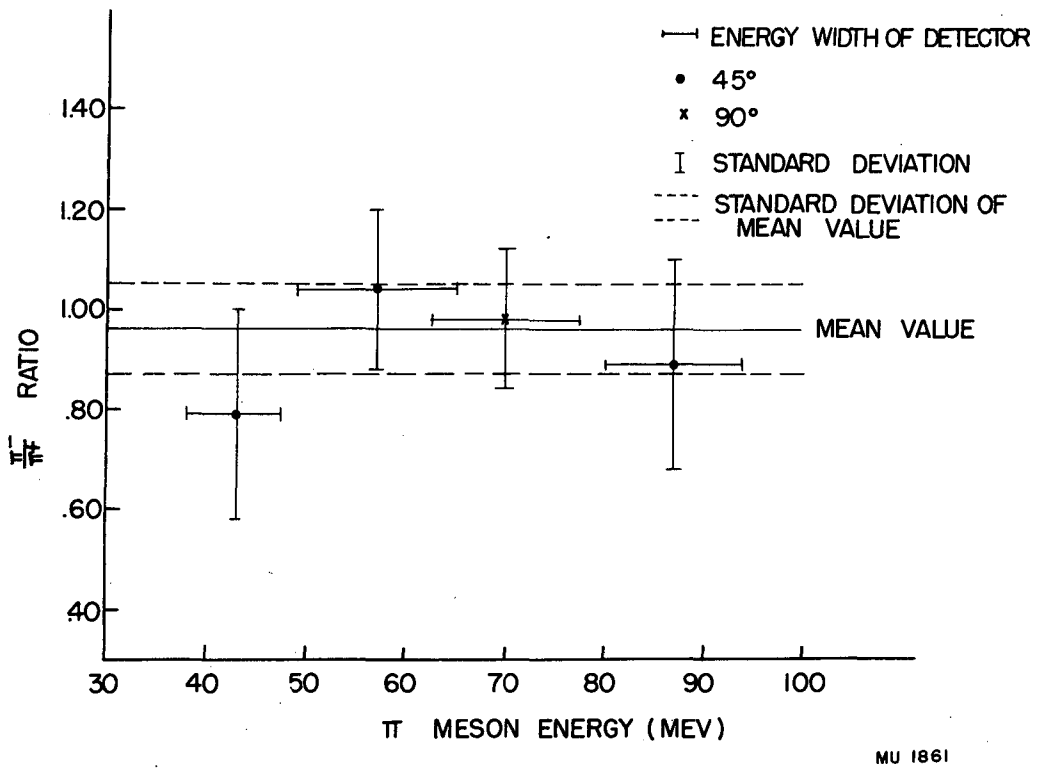
ENERGY WIDTH OF DETECTOR
45°
90°
STANDARD DEVIATION
STANDARD DEVIATION OF MEAN VALUE
MEAN VALUE
1.40
1.20
1.00
.80
.60
.40
RATIO
30
40
50
60
70
80
90
100
π MESON ENERGY (MEV)
MU 1861

Fig. 16

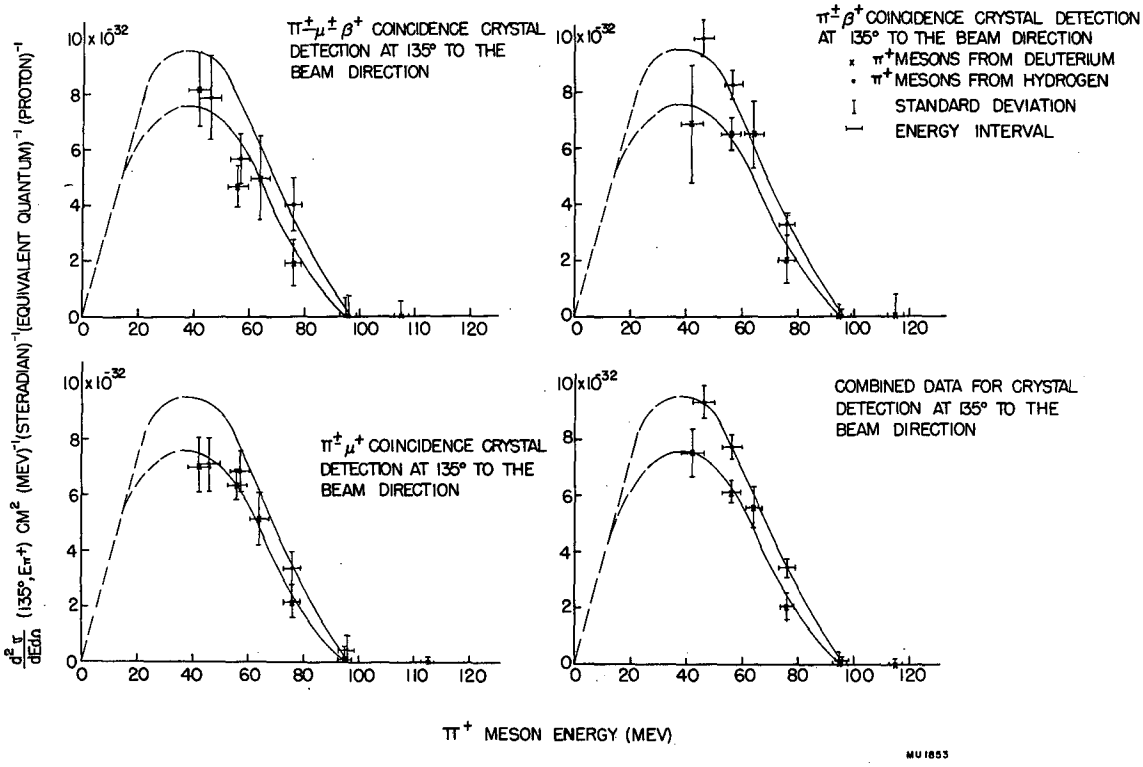
$\pi^{\pm}\mu^{\pm}\beta^{+}$ COINCIDENCE CRYSTAL DETECTION AT 135° TO THE BEAM DIRECTION
$\pi^{\pm}\beta^{+}$ COINCIDENCE CRYSTAL DETECTION AT 135° TO THE BEAM DIRECTION
π^{+} MESONS FROM DEUTERIUM
π^{+} MESONS FROM HYDROGEN
STANDARD DEVIATION
ENERGY INTERVAL
$\pi^{\pm}\mu^{+}$ COINCIDENCE CRYSTAL DETECTION AT 135° TO THE BEAM DIRECTION
COMBINED DATA FOR CRYSTAL DETECTION AT 135° TO THE BEAM DIRECTION
$\frac{d^2\sigma}{d\Omega dn}$ (135°, E_{π^+}) CM^2 (MEV)$^{-1}$(STERADIAN)$^{-1}$(EQUIVALENT QUANTUM)$^{-1}$ (PROTON)$^{-1}$
π^+ MESON ENERGY (MEV)
MU 1853

Fig. 17

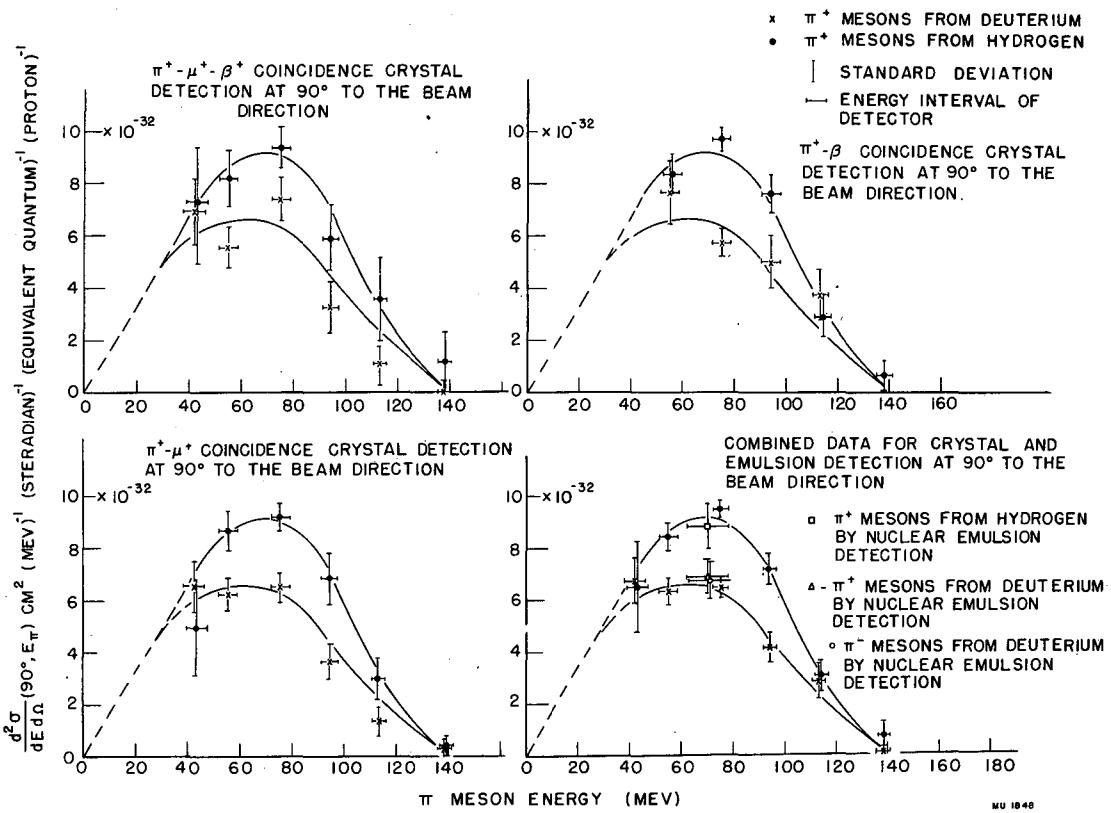
x π+ MESONS FROM DEUTERIUM
• π+ MESONS FROM HYDROGEN
STANDARD DEVIATION
ENERGY INTERVAL OF DETECTOR
π+-β COINCIDENCE CRYSTAL DETECTION AT 90° TO THE BEAM DIRECTION.
π+-μ+-β+ COINCIDENCE CRYSTAL DETECTION AT 90° TO THE BEAM DIRECTION
π+-μ+ COINCIDENCE CRYSTAL DETECTION AT 90° TO THE BEAM DIRECTION
COMBINED DATA FOR CRYSTAL AND EMULSION DETECTION AT 90° TO THE BEAM DIRECTION
□ π+ MESONS FROM HYDROGEN BY NUCLEAR EMULSION DETECTION
△ - π+ MESONS FROM DEUTERIUM BY NUCLEAR EMULSION DETECTION
○ π− MESONS FROM DEUTERIUM BY NUCLEAR EMULSION DETECTION
× 10−32
d²σ/dE dΩ (90°, Eπ) CM² (MEV)⁻¹ (STERADIAN)⁻¹ (EQUIVALENT QUANTUM)⁻¹ (PROTON)⁻¹
π MESON ENERGY (MEV)
MU 1848

Fig. 18

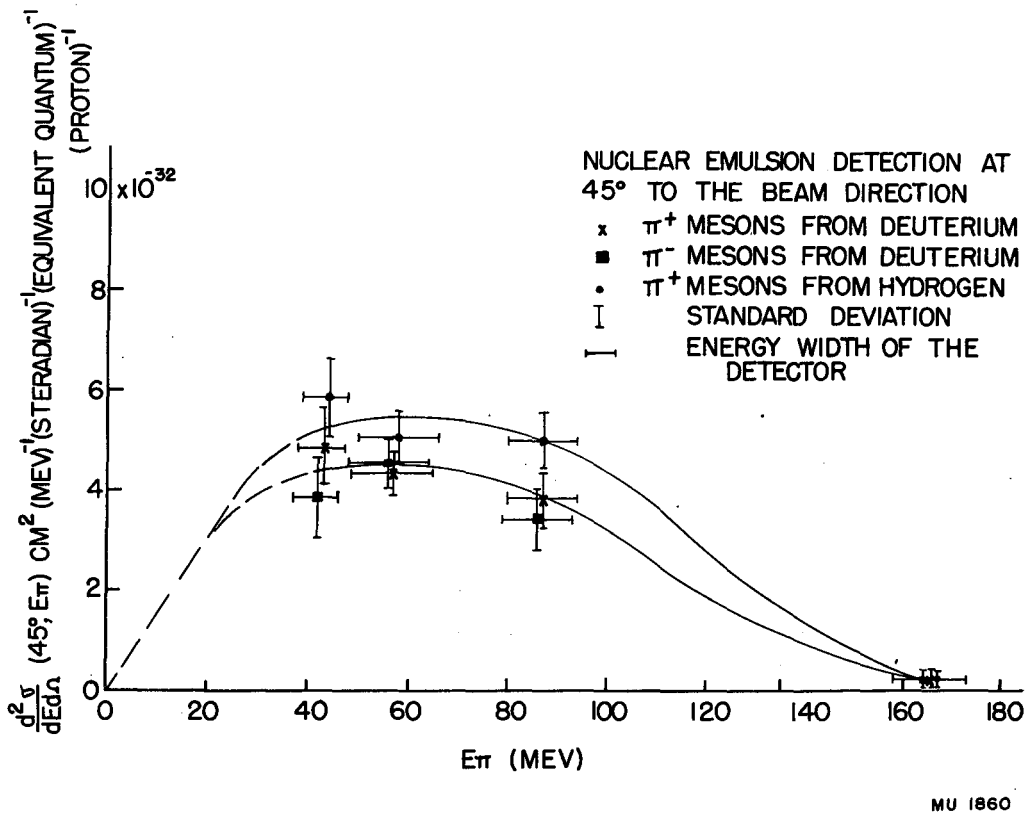
NUCLEAR EMULSION DETECTION AT
45° TO THE BEAM DIRECTION
x π+ MESONS FROM DEUTERIUM
■ π- MESONS FROM DEUTERIUM
• π+ MESONS FROM HYDROGEN
STANDARD DEVIATION
ENERGY WIDTH OF THE DETECTOR
d²σ/dEdΩ (45°, Eπ) CM² (MEV)⁻¹(STERADIAN)⁻¹(EQUIVALENT QUANTUM)⁻¹ (PROTON)⁻¹
10 x10⁻³²
8
6
4
2
0
0
20
40
60
80
100
120
140
160
180
Eπ (MEV)
MU 1860

Fig. 19

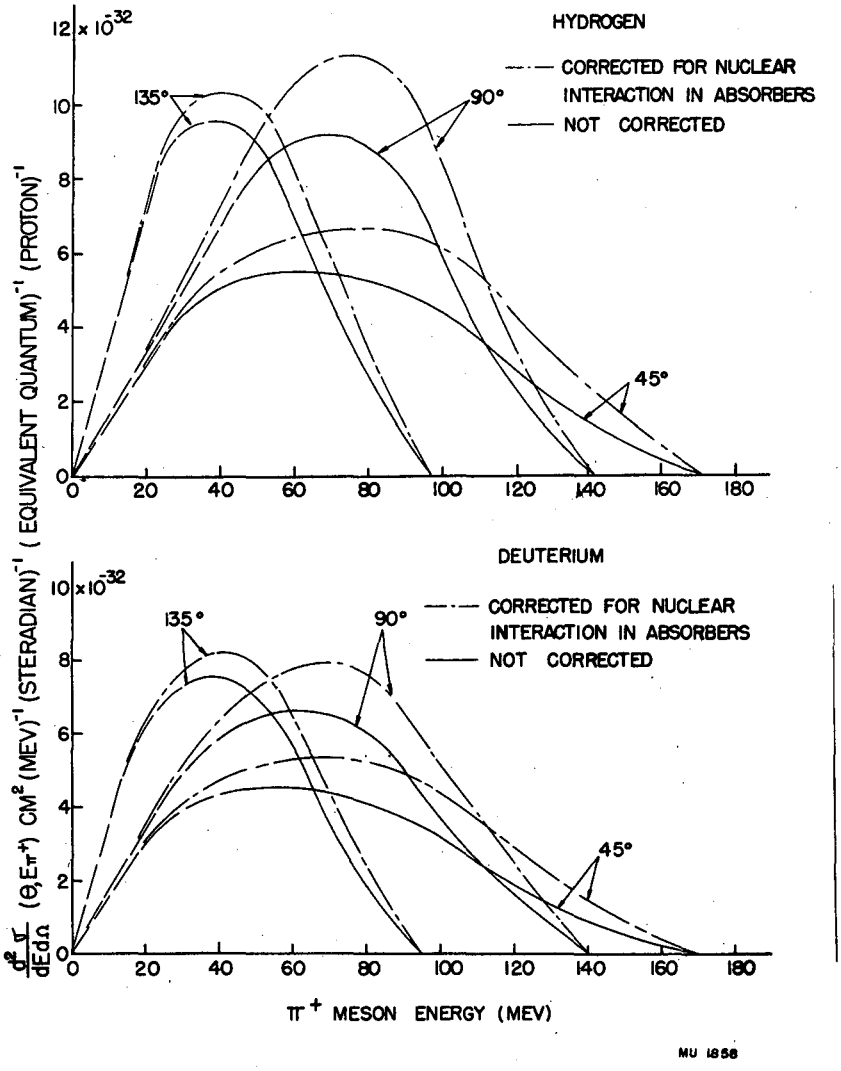
HYDROGEN
CORRECTED FOR NUCLEAR INTERACTION IN ABSORBERS
NOT CORRECTED
135°
90°
45°
12 x 10^-32
10
8
6
4
2
0
0
20
40
60
80
100
120
140
160
180
DEUTERIUM
10 x 10^-32
CORRECTED FOR NUCLEAR INTERACTION IN ABSORBERS
NOT CORRECTED
135°
90°
45°
d²σ/dEdΩ (θ,Eπ+) CM² (MEV)⁻¹ (STERADIAN)⁻¹ (EQUIVALENT QUANTUM)⁻¹ (PROTON)⁻¹
π+ MESON ENERGY (MEV)
MU 1858

Fig. 20

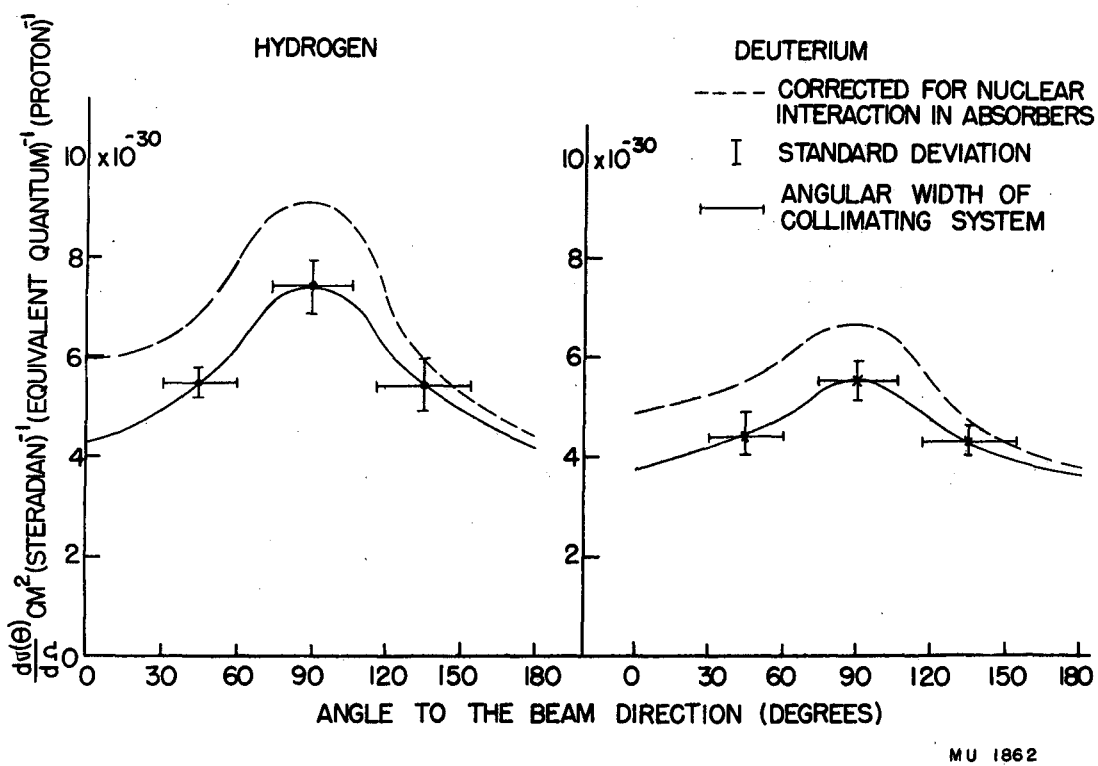
HYDROGEN
DEUTERIUM
CORRECTED FOR NUCLEAR INTERACTION IN ABSORBERS
STANDARD DEVIATION
ANGULAR WIDTH OF COLLIMATING SYSTEM
$\frac{d\sigma(\theta)}{d\Omega}$ CM^2 (STERADIAN)$^{-1}$ (EQUIVALENT QUANTUM)$^{-1}$ (PROTON)$^{-1}$
10 x10^{-30}
8
6
4
2
0
0 30 60 90 120 150 180
ANGLE TO THE BEAM DIRECTION (DEGREES)
MU 1862

Fig. 21

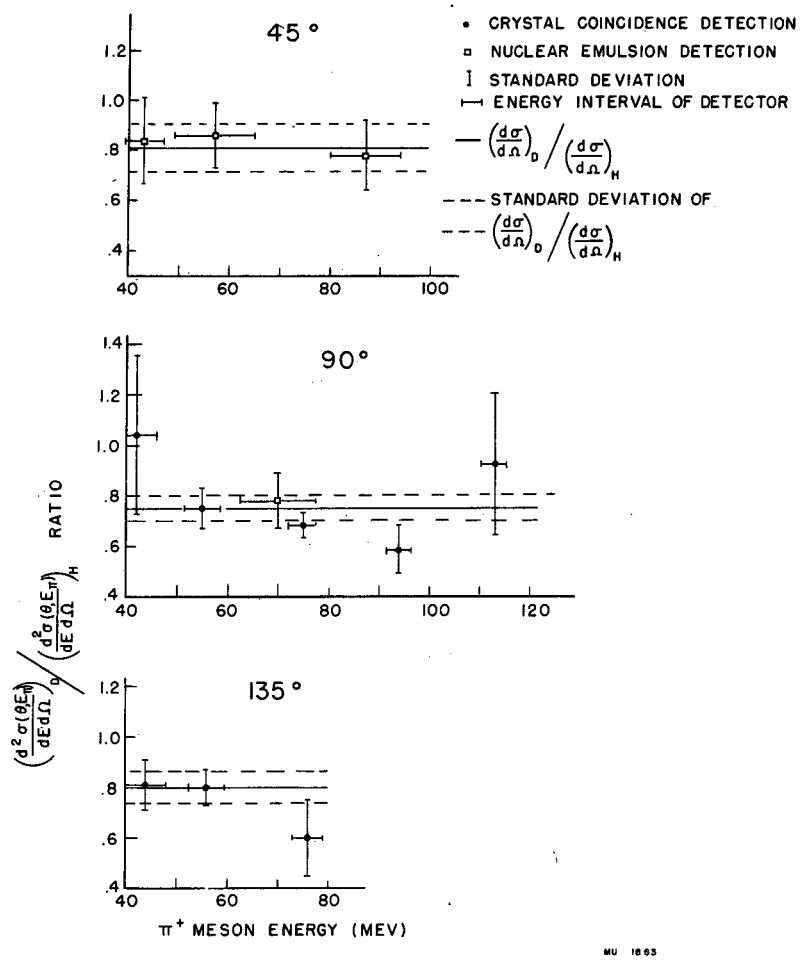
45°
90°
135°
• CRYSTAL COINCIDENCE DETECTION
▫ NUCLEAR EMULSION DETECTION
I STANDARD DEVIATION
⊢⊣ ENERGY INTERVAL OF DETECTOR
— $\left(\frac{d\sigma}{d\Omega}\right)_D \Big/ \left(\frac{d\sigma}{d\Omega}\right)_H$
--- STANDARD DEVIATION OF
--- $\left(\frac{d\sigma}{d\Omega}\right)_D \Big/ \left(\frac{d\sigma}{d\Omega}\right)_H$
$\left(\frac{d^2\sigma(\theta E_\pi)}{dE\,d\Omega}\right)_D \Big/ \left(\frac{d^2\sigma(\theta E_\pi)}{dE\,d\Omega}\right)_H$ RATIO
π^+ MESON ENERGY (MEV)
MU 1865

Fig. 22

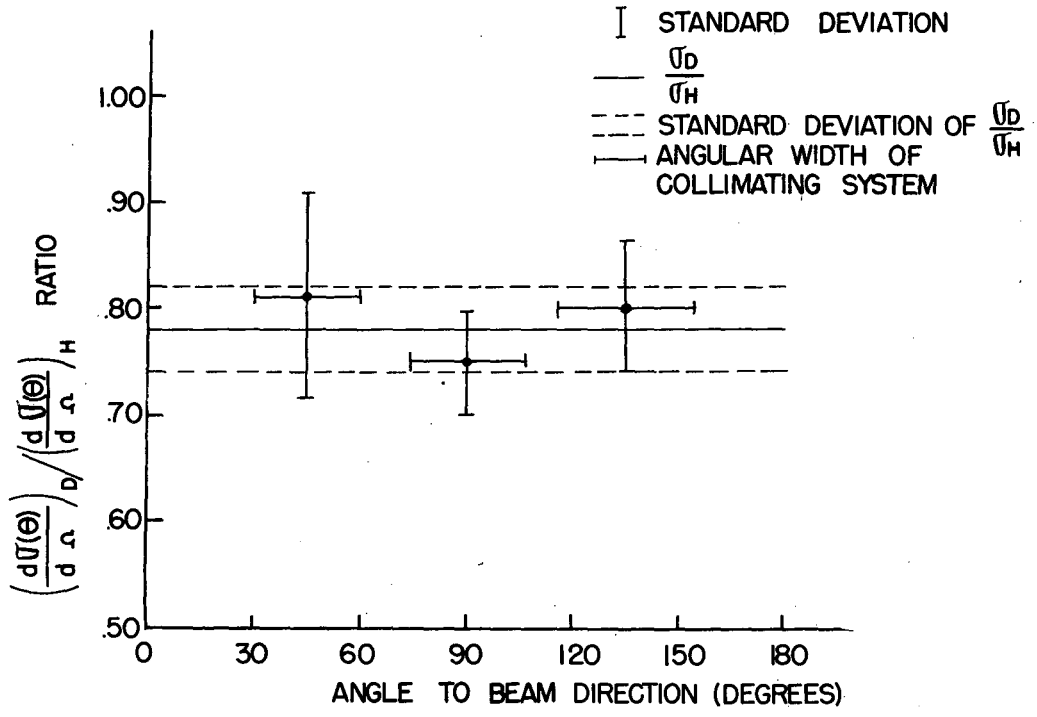
STANDARD DEVIATION
$\frac{\sigma_D}{\sigma_H}$
STANDARD DEVIATION OF $\frac{\sigma_D}{\sigma_H}$
ANGULAR WIDTH OF COLLIMATING SYSTEM
$\left(\frac{d\sigma(\theta)}{d\Omega}\right)_D / \left(\frac{d\sigma(\theta)}{d\Omega}\right)_H$ RATIO
1.00
.90
.80
.70
.60
.50
0
30
60
90
120
150
180
ANGLE TO BEAM DIRECTION (DEGREES)
MU 1857

Fig. 23